MINERALOGY AND GEOCHEMISTRY OF THE SOUTHERN AMETHYST VEIN SYSTEM, CREEDE MINING DISTRICT, COLORADO

by

Mark P. Hemingway

Submitted in Partial Fulfillment
of the Requirements for the Degree of
Master of Science in Geology

New Mexico Institute of Mining and Technology

Socorro, New Mexico

March, 1986

ACKNOWLEDGEMENTS

This work would have been impossible without the assistance and cooperation of the Pioneer Nuclear Corporation. The special contributions of Richard Robinson and Paul Eimon are noted with gratitude.

Research was funded in part by a grant from Sigma Psi.

The guidance and aid of David Norman and Andrew Campbell were crucial in the development and culmination of this project. Their willing attitudes, expertise and interest improved the quality of this research beyond measure, and are greatly appreciated.

Recognition must also be extended to the New Mexico Bureau of Mines and Mineral Resources for providing the employment which permitted this effort to proceed. In particular, the support and understanding of Gary Johnpeer and David Love were invaluable. In addition, the assistance of Lynn Brandvold in the determination of metal concentrations was most helpful.

Without the companionship and cheer provided by the pack of rabble-rousing scum I have been unfortunate enough to call my friends, insanity and brain death would have been inevitable. For their help in easing the frustration and tension of the past year, I thank them all.

Most importantly, it is necessary to acknowledge the three people most strongly responsible for the completion of this research: my parents and my fiancee. Without their constant warmth, love, and encouragement, there would have been no motivation for completion.

ABSTRACT

The Creede mining district is a collection of epithermal Ag-Au-base metal deposits in southwestern Colorado. A mineralogic, paragenetic, fluid inclusion, and geochemical investigation was perfomed on samples from the 375 m of vertical section of the southern Amethyst vein system, which has been one of the most productive areas within the district. This study was undertaken in order to better define the nature of the mineralizing system.

Mineralization within the study area occurs both within veins and as fine disseminations within country rock proximal to veins. Veins are typically finely-laminated quartz, although barite, rhodochrosite, manganese oxides, and hematite are also common. Sulfides are fine-grained, averaging 0.5 to 1 mm in diameter, and occur as discrete blebs with a wide variety of intergrowths. Textures indicating replacement are quite common, and suggest that replacement was sequential in the order sphalerite to galena to chalcopyrite to accanthite to sulfosalts (undivided) to covellite. Pyrite and tetrahedrite were also present, but could not be precisely placed within this sequence.

Limited fluid inclusion analyses and metal concentration values displayed significant variation with elevation. Homogenization temperatures and salinities were observed to decrease with increasing elevation within the vein system. Lead and zinc values are highest at the base of the system, and decrease upwards. Silver, however, is highest at upper elevations, coinciding with the increasing abundance of acanthite and argentiferous sulfosalts. Silver is present at lower elevations, but occurs mainly as solid solution within galena and copper sulfides. Manganese and iron concentrations are also highest at the top of the system.

Geochemical calculations indicate that the sulfide replacement sequence would have resulted from a simultaneous decrease in temperature and increase in f_{O_2} of the ore solutions. Mineralogic considerations indicate that these parameters may have been varying in a cyclical manner. These data are best explained by the presence of a stacked-cell convection system within the southern Amethyst vein system. Under such a system, cool, dilute surface waters convected in a cell overlying the circulating ore fluids, and most mineralization took place at the zone of mixing between the cells. Repeated vertical movement of this mixing zone would have produced the cyclical pattern observed in vein mineralization.

The rarity of acanthite at lower elevations within the vein system may be due to undersaturation of silver relative to lead entering the system. Calculations indicate that acanthite should not have been precipitated until reaching fluid conditions present only in the upper elevations of the vein system. Estimations of molar Ag/Pb ratio for solutions entering the vein system suggest that lead concentrations should have been approximately 11 times those of silver.

Similar replacement sequences to those presented here are observed in other epithermal deposits. Since this sequence indicates a rapid temperature decrease, fluid mixing may have been an active part of the mineralization process in these deposits. This specific sequence might prove useful as an indicator of rapid cooling in other deposits.

Table of Contents

INTRODUCTION

The San Juan volcanic field of southern Colorado and northern New Mexico is the largest remnant of an expanse of volcanic and associated intrusive and sedimentary rocks which dominated the southern Rocky Mountains during the late Tertiary (Lipman, 1975). The volcanic field hosts numerous epithermal deposits, the most intensely studied of which is the Creede mining district, an epithermal Ag-base metal deposit in the central part of the volcanic field (fig. 1). Although most of the published research on the district has been concentrated on the more accessible OH vein system (Roedder, 1960; Barton et al., 1971; Bethke and Barton, 1971; Bethke et al., 1973; Roedder, 1974; Steven and Eaton, 1975; Bethke et al., 1976; Barton et al., 1977; Bethke and Rye, 1979; Doe et al., 1979; Giudice, 1980), some of the highest silver values have come from the southern end of the Amethyst vein system (fig. 2) (Robinson and Norman, 1984). It has been proposed in several previous studies (Barton et al., 1977; Berger and Eimon, 1981; Robinson and Norman, 1984) that surface waters might have mixed with ore solutions during mineralization of the southern Amethyst vein system. Robinson and Norman (1984) present evidence which strongly suggest that the southern one-third of the Amethyst vein system may have been a zone of active mixing, and that the high metal values of

Figure 1. Location map of known calderas and the Creede mining district within the San Juan volcanic field of Colorado. Calderas shown are:

B -Bachelor

Bz -Bonanza

C -Creede

CP -Cochetopa Park

L -Lost Lake

LC -Lake City

LG -La Garita

M -Mammoth Mountain

MH -Mount Hope

P -Platoro

S -Silverton

SJ -San Juan

SL -San Luis

SM -Summitville

U -Ute Creek

UN -Uncompahgre

Modified from Steven and Eaton (1975).

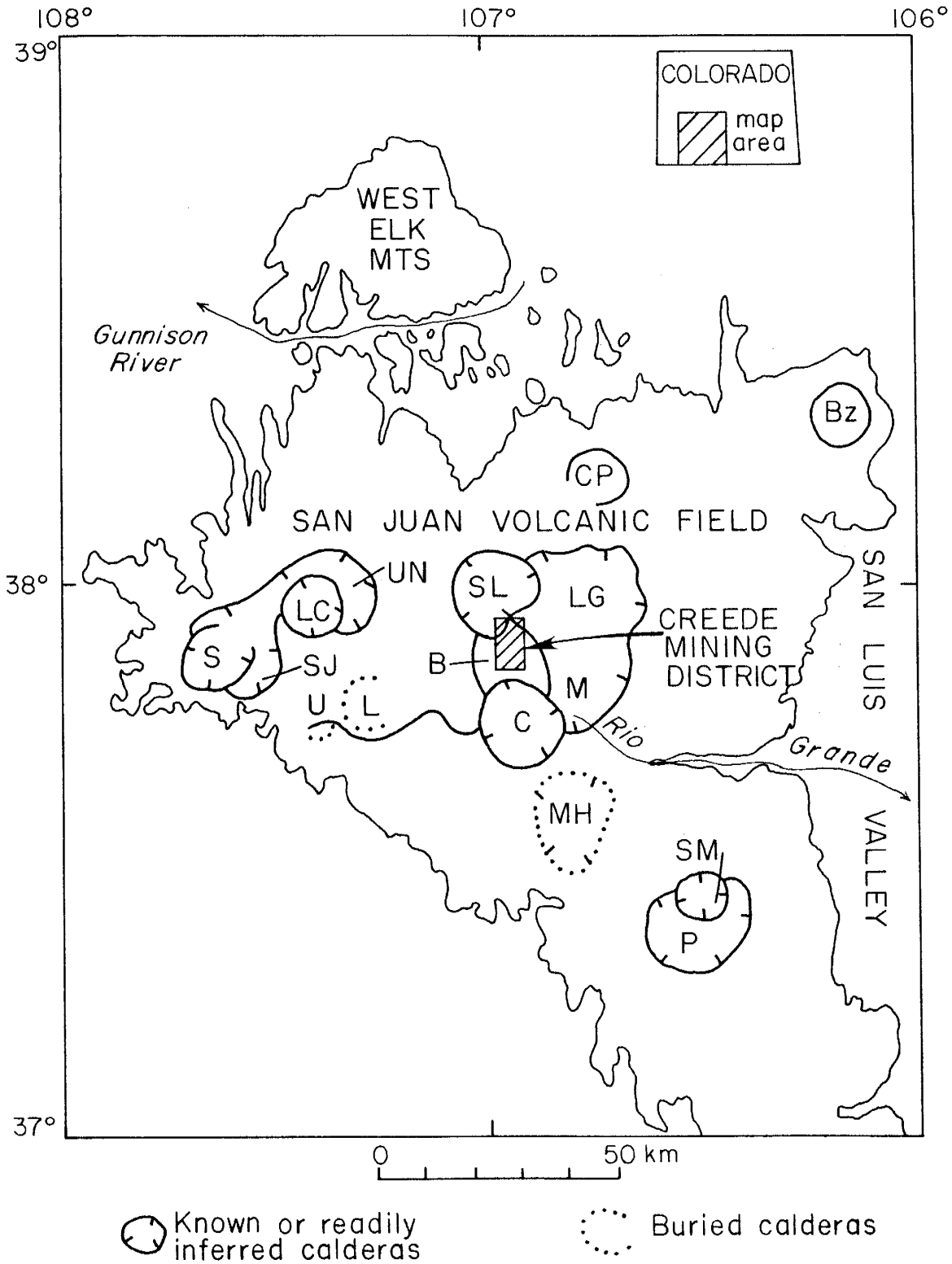
108°
107°
106°
39°
38°
37°
COLORADO
map area
WEST ELK MTS
Gunnison River
Bz
CP
SAN JUAN VOLCANIC FIELD
SAN LUIS VALLEY
UN
SL
LG
LC
CREEDE MINING DISTRICT
S
SJ
B
M
U
L
C
Rio Grande
MH
SM
P
0
50 km
Known or readily inferred calderas
Buried calderas

Figure 2. Major mineralized structures within the Creede mining district. The north-south oriented structures form the keystone graben discussed in the text. Northeast-southwest and east-west oriented structures in the southern part of the map area form the bounding faults of the Creede caldera. Modified from Steven and Eaton (1975).

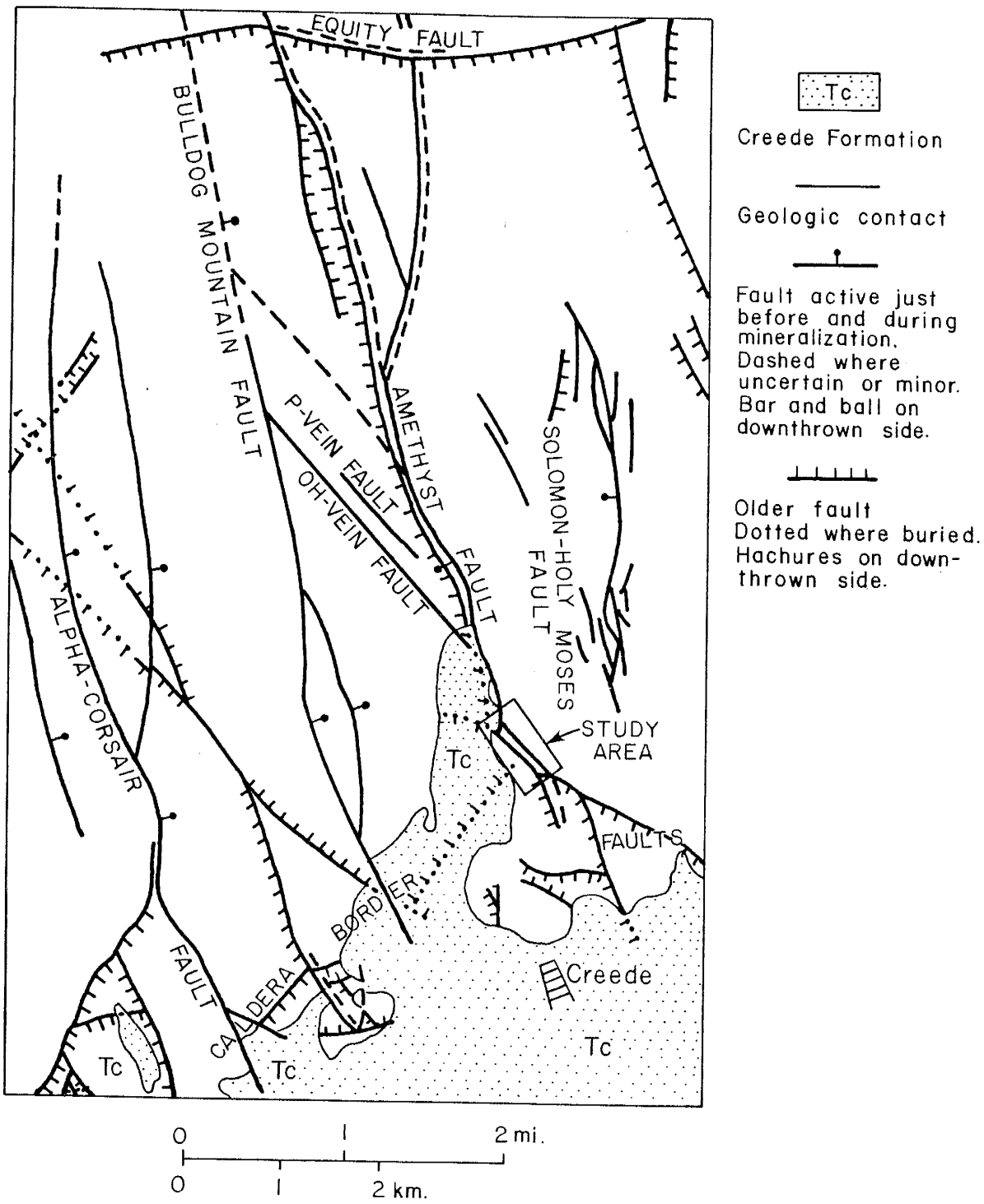
EQUITY FAULT
BULLDOG MOUNTAIN FAULT
P-VEIN FAULT
OH-VEIN FAULT
AMETHYST FAULT
SOLOMON-HOLY MOSES FAULT
ALPHA-CORSAIR
STUDY AREA
FAULTS
BORDER
FAULT
CALDERA
Creede
Tc
Tc
Tc
Tc
Tc
Creede Formation
Geologic contact
Fault active just before and during mineralization. Dashed where uncertain or minor. Bar and ball on downthrown side.
Older fault Dotted where buried. Hachures on downthrown side.
0 1 2 mi.
0 1 2 km.

this area may in fact be a relict of such mixing.

The purpose of this investigation was to better define the chemical nature of the mineralizing system active within the southern Amethyst vein system. Of particular interest was characterization of the geochemical system responsible for mineralization in light of the strong evidence from previous studies for the mixing of two distinct fluids.

Methods of Investigation

Samples were taken from both drill core and underground exposures throughout the 375 m vertical section of the southern Amethyst vein system. Mineralogic samples were examined using relected light microscopy; this was supplemented by scanning electron microscopy in conjunction with an EDS semi-quantitative elemental analyser. Homogenization and freezing temperatures for fluid inclusions in selected samples were determined in order to correlate with the fluid inclusion study performed by Robinson and Norman (1984). Concentrations of Pb, Zn, Ag, Cu, Fe, and Mn for vein samples were determined using atomic absorption analysis.

GEOLOGIC SETTING

The San Juan volcanic field began with the widespread Oligocene eruption of andesitic lavas at approximately 35 Ma (Lipman,1979). Approximately 30 Ma, the character of volcanism changed, apparently in response to the intrusion of a series of relatively high level, very silicic stocks. Pyroclastic eruptions replaced andesitic lavas as the primary form of volcanic activity, resulting in the formation of sixteen to seventeen calderas within the field (fig. 1).

The following sequence of events is summarized from Steven and Eaton (1975). In the Bachelor caldera of the central San Juans, eruption of the Carpenter Ridge Tuff was followed by resurgence of the central dome of the caldera. Extensional stresses induced by this resurgent doming resulted in the formation of a keystone graben which extended across the north-northwest axis of the dome (see fig. 2), and intersected the fanglomerates of the moat-filling Creede formation at its southern extent. The normal faults related to graben formation were typically high-angle, with displacements up to a few hundred meters on major structures. Dilations resulting from this faulting and from associated fracturing and brecciation provided the infrastructure for later hydrothermal mineralization.

Mineralization slightly post-dates most of the movement on faults in the district (Robinson and Norman, 1984). Within the OH vein system, K-Ar dating of alteration minerals indicates that mineralization took place at 24.6 +/- 0.6 Ma (Bethke et al., 1976); geochemical calculations indicate that mineralization processes may have been active for only a few thousand years (Barton et al., 1977). The lead in sulfides from the OH vein system is indicated by lead isotopic data (Doe et al., 1979) to have been derived from the preCambrian basement (or sediments derived from it) which is believed to underlie the district.

The mineralized structures within the study area, both including and associated with the major Amethyst vein, occur with great density and form a complex network of interconnecting veins. The Amethyst vein is the largest observed in the system, with widths up to 6 m reported (Robinson and Norman, 1981). Vein widths vary from this maximum to a minimum of less than 500 u observed for some microveinlets.

Both Robinson and Norman (1984) and Giudice (1980) provide detailed descriptions of vein morphology. Prominent features include warped fault planes, localized intense brecciation, anastomosing veins, cymoid loops, and abrupt variations in the attitude and size of smaller veins (<30 cm width). These same

smaller veins are reported to have very limited lateral and vertical extent.

The hydrologic system which developed in this infrastructure has been postulated by Bethke and Rye (1979) to have been primarily charged with meteoric waters. Carbon, hydrogen, and oxygen isotope data indicates that these waters were derived from two sources, and may have contained a minor magmatic constituent. According to Barton et al. (1977), these solutions were circulating to an unknown depth below the paleosurface, then convecting freely upwards and to the south through the network of interconnecting fault and fracture systems, mineralizing structures as they moved. The nature of the heat source driving convection is uncertain, but the presence of a stock below the mineralized area has been postulated on the basis of gravity studies of the district (Steven and Eaton, 1975). Heat from this stock, if present, may have been the cause of hydrothermal circulation within the deposit.

Barton et al. (1977) have calculated several fluid parameters for the OH vein system at the time of ore deposition based on fluid inclusion analyses and mineral associations and geochemistry. They conclude, briefly, that the fluid had temperatures of 250^{o}C, a pH of 5.4, a salinity of approximately 1 molal, and a log f_{O_2} of

approximately -35 (frequently fluctuating). If fluids were migrating southward, ore solutions with these approximate characteristics would have entered the southern Amethyst vein system at the northern end of the study area.

MINERALIZATION

Types and Style

Two types of mineralization were observed within the part of the Southern Amethyst vein system examined; they are vein mineralization formed by sequential layering of gangue minerals (dominantly silica) with metallic sulfides and oxides, and fine-grained disseminations of ore minerals in country rock.

Gangue minerals within the veins typically form a series of fine layers or laminations parallel to sub-parallel to the vein margins (fig. 3). These layers vary from approximately 0.5 mm to more than 2 cm in width, and are discontinuous laterally and vertically. In addition, both the sequence of mineralization and the suite of minerals present in any given vein are quite variable, rendering correlation between even closely spaced samples impossible. Most of this gangue mineralization is as any of a number of forms of silica, including clear and amythestine prismatic quartz and clear to milky chalcedony. Most veins observed are composed of more than one of these forms, often in an alternating style. Crystalline barite and microcrystalline rhodochrosite and manganese oxides are common vein-forming gangue minerals locally.

Figure 3. Photograph of sample of vein material, illustrating finely-banded style typical of mineralization.

a) Interlayered crystalline and cryptocrystalline quartz and barite. Sample 5014.

b) Polished sections of ore material. Note fine layering of each sample and symmetrical fine laminae of hematite (red) in sample on left. Samples 5006 (left), 5024C (right).

Sulfides observed are galena, sphalerite, chalcopyrite, pyrite, acanthite, covellite, tetrahedrite, lead sulfosalts (undivided), and alabandite. These occur as discrete and intergrown crystals up to approximately 0.5 cm in diameter. Most are quite fine, averaging 1 to 2 mm in diameter, and are typically subhedral. Sulfides occur both within and between crystals and layers of gangue minerals, but in any locality generally are concentrated within only a few layers. The sulfide mineralogy varies considerably, between both different layers and different samples.

EDS elemental analysis (detection limit 0.1 wt.% Ag) found galena, chalcopyrite, covellite, and the sulfosalts to contain variable amounts of silver, perhaps present as small disseminated inclusions or in solid solution. The sulfosalts consist of lead, arsenic, and sulfur, with variable amounts of antimony.

Hematite is quite common and occurs in a variety of forms; as intergrowths with sulfide minerals, particularly covellite, as subspherical aggregates present within crystalline quartz (fig. 4). and in thin, often discontinuous bands between some layers of vein silica (fig 3.b.).

Disseminated mineralization occurs as grains up to approximately 0.5 mm in diameter hosted within open spaces in the country rock, typically in proximity to

Figure 4. SEM photomicrograph of subspherical aggregates of hematite (light-colored material) included within crystalline vein quartz (dark-colored material). Sample 5030, 2500x.

veins. All sulfide and oxide phases observed within veins were also present as disseminations. The typical hosts for this mineralization are highly porous, unflattened pumice fragments. Although visible silver mineralization was not observed in the samples of disseminated mineralization studied, high silver values are reputed to have been obtained from ore of this type (Giudice, 1980).

Sulfide Paragenesis

Most sulfide grains display one or more types of intergrowth textures, either with other sulfides or with iron oxides. Most of these intergrowths are interpreted to indicate the replacement of one phase by another. Examples of observed textures that display a clear temporal relationship between phases are cores of one mineral surrounded by reaction rims of another, inclusions of one mineral within another, crenulated margins between sulfide phases (caries texture), and cross-cutting structures (Colony, 1928; Bastin et al., 1931).

The observed replacement sequence is sphalerite to galena to chalcopyrite to acanthite to lead sulfosalts (undivided) to covellite (fig. 5). Mineral phases may replace all those listed before them; e.g. acanthite is observed replacing sphalerite, galena, and chalcopyrite. In addition to the listed sequence,

Figure 5. Light and SEM photomicrographs illustrating the sequence of sulfide replacement, and many of the typical textures involved in replacement.

a) Galena grain with a replacement rim of acanthite (light gray), sulfosalts (dark gray), and covellite (blue). Sample 5025, 50x.

b) SEM photomicrograph detail of grain tip shown in photo 5.a. Note sequential replacement of the central galena (white) by (in order) acanthite (dark gray), sulfosalts (light gray), and covellite (very dark gray). This photomicrograph was taken with the SEM in a back-scattering mode, so that the brightness of minerals shown is proportional to their molecular weight. Sample 5025, 50 u bar for scale.

Figure 5. (cont.)

c) Galena (white) replaced by sulfosalts and covellite. Sulfosalts are also being replaced by covellite. Sample 5013, 200x.

d) Sphalerite (dark gray) replaced by galena (white) replaced by chalcopyrite (yellow). Sample 5009, 200x.

Figure 5. (cont.)

e) Sphalerite (dark gray) replaced by galena (white). Sample 5024A, 100x.

f) Galena (white) with a replacement rim of acanthite replaced by sulfosalts (grey). All three minerals are being replaced by the cross-cutting needles of covellite (blue). Sample 5008A, 100x.

Figure 5. (cont.)

g) Galena (white) replaced by chalcopyrite (yellow) and sulfosalts (gray). All three minerals are replaced by covellite (blue). Sample 5025, 100x.

pyrite is replaced by chalcopyrite, although the fine-grained nature of pyrite and the absence of temporally definitive intergrowths with other sulfides preclude a more exact placement within the sequence. Tetrahedrite and alabandite also exhibit intergrowth textures, but could not be placed in the replacement sequence due to rarity of occurrence. Hematite replaces all sulfide minerals.

Few mineral grains exhibit the entire replacement sequence. Observed replacements were, however, always in the order given. Significantly, this sequence was observed within several different layers within the same samples. In contrast, disseminated minerals exhibit the same sequence of replacement as vein sulfides, but without any indication of having been repeated. Robinson and Norman (1984) present a complex paragenesis for the study area, based primarily on field relations. An overall mineral paragenesis is submitted within the framework of two basic stages of mineralization. Since the paragenesis here presented was derived primarily from laboratory study, it was not possible to correlate closely with these mineralization stages. Despite this the paragenesis here presented agrees in broad outline that of the earlier study. Although Robinson and Norman place galena before sphalerite in the overall sequence of mineralization, this is the only major contrast between the two paragenetic series.

Vertical Distribution of Minerals

Although the paragenesis is applicable throughout the entire vein system, the abundance of specific minerals and textures varies considerably with elevation through the 375 m of section examined (fig. 6). In the upper part of the system (above 10,000 ft. or 3,000 m elevation), acanthite and sulfosalts are common. Here, the base metal sulfides are predominantly galena, sphalerite, and covellite; chalcopyrite and pyrite are of rare occurrence. The particular replacement sequence of galena to acanthite to sulfosalts, all crosscut by needles of covellite, is seen only in these elevations. Disseminated mineralization in the upper half of the system is primarily iron and manganese oxides; disseminated sulfides are of rare occcurrence. Manganese mineralization occurs only as oxides; no carbonates were observed. In the upper 200 m of the vein system, quartz crystals were observed to occur with intracrystalline subspherical inclusions of hematite which appear to be of a primary origin.

In the lower half of the system, base metal sulfides are predominant, and acanthite and sulfosalts are extremely rare. Galena and sphalerite are the most common sulfides, occurring in greater abundance than in the upper elevations. Covellite, chalcopyrite, and pyrite, however, are common, and are approximately 25%

Figure 6. Variation in mineral abundance with elevation. Band widths represent general variations in relative mineral abundances. Note the greater abundance of minerals associated with more oxidizing conditions (e.g., hematite, manganese oxides, covellite) above approximately 3,000 m elevation.

meters
3,100
3,000
2,900
2,800
BARITE
RHODOCHROSITE
MANGANESE OXIDES
HEMATITE
COVELLITE
SULFOSALTS
ACANTHITE
PYRITE
CHALCOPYRITE
SPHALERITE
GALENA
feet
10,400
10,000
9,600
9,200

(by volume) of the total observed sulfides. Rhodochrosite and alabandite are observed only within the lower half of the system, and manganese oxides are much less abundant than above. Disseminated mineralization consists of covellite, chalcopyrite, hematite and pyrite, with lesser amounts of other sulfides. Intergrowths of covellite and hematite are very common.

GEOCHEMISTRY

Metal Concentrations

The concentrations of Pb, Zn, Cu, Ag, Fe, and Mn were determined by atomic absorption methods for 25 samples of vein material from various levels (fig. 7). The results of analysis broadly mimic the mineralogical variations observed. Lead values decrease with increasing elevation, while silver behaves in an opposite fashion. Silver was present at lower elevations, despite the rarity of silver minerals. EDS analysis indicates that it is present at these levels mainly as solid solution within the galena, covellite, and chalcopyrite.

Manganese values also increase with increasing elevation, although not so strongly as those of silver. Iron concentrations vary little with elevation, except at the highest elevations sampled (10,360 ft. elevation), where values as high as 6 wt. % are observed. For copper and zinc, no distinct variations with elevation are observed.

Fluid Inclusions

Samples and sample locations differed from those of Robinson and Norman (1984). For this reason,

Figure 7. Metal concentrations vs. elevation for mine and drill core samples. Concentrations were determined using atomic absorption analytical techniques.

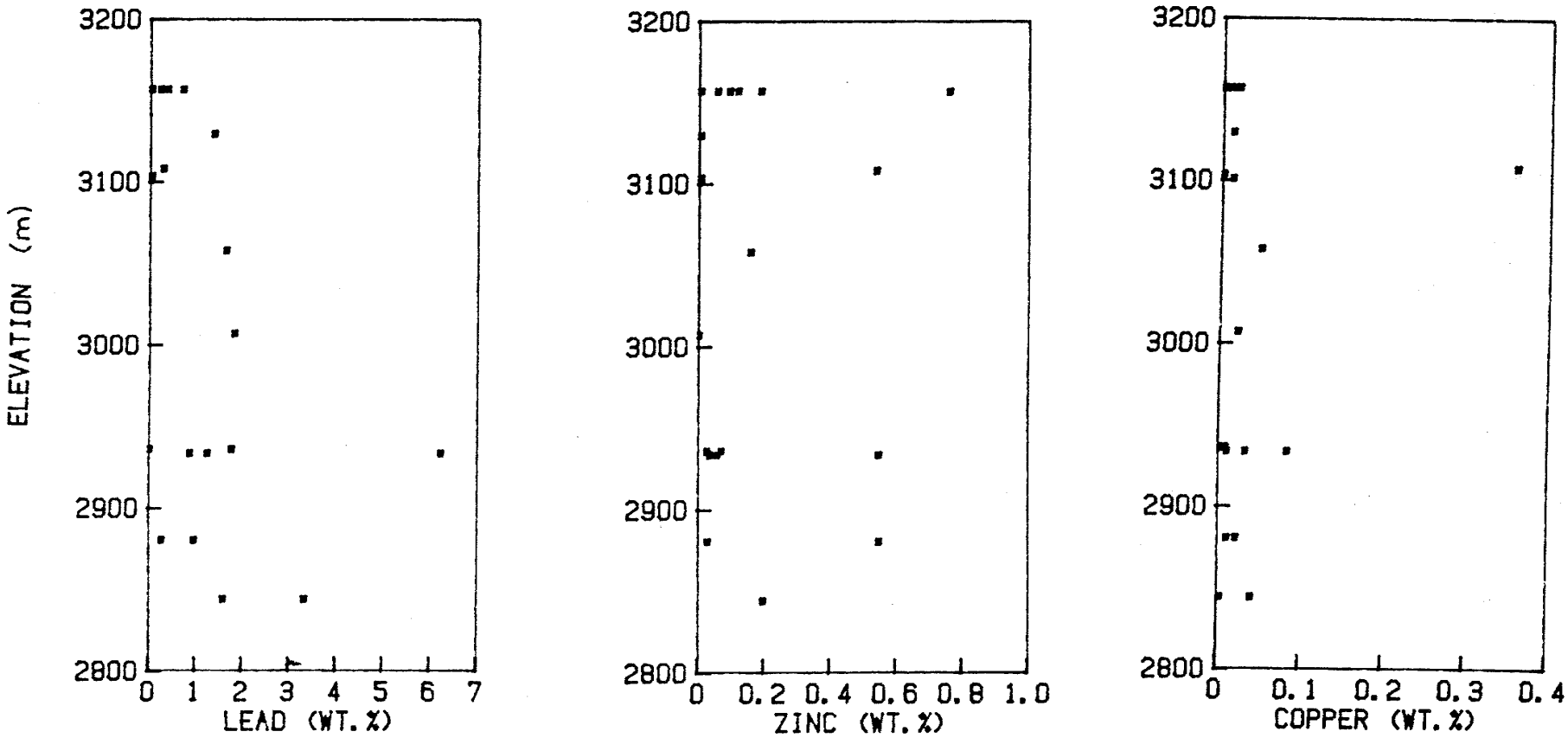
ELEVATION (m)
3200
3100
3000
2900
2800
0 1 2 3 4 5 6 7
LEAD (WT.%)
0 0.2 0.4 0.6 0.8 1.0
ZINC (WT.%)
0 0.1 0.2 0.3 0.4
COPPER (WT.%)

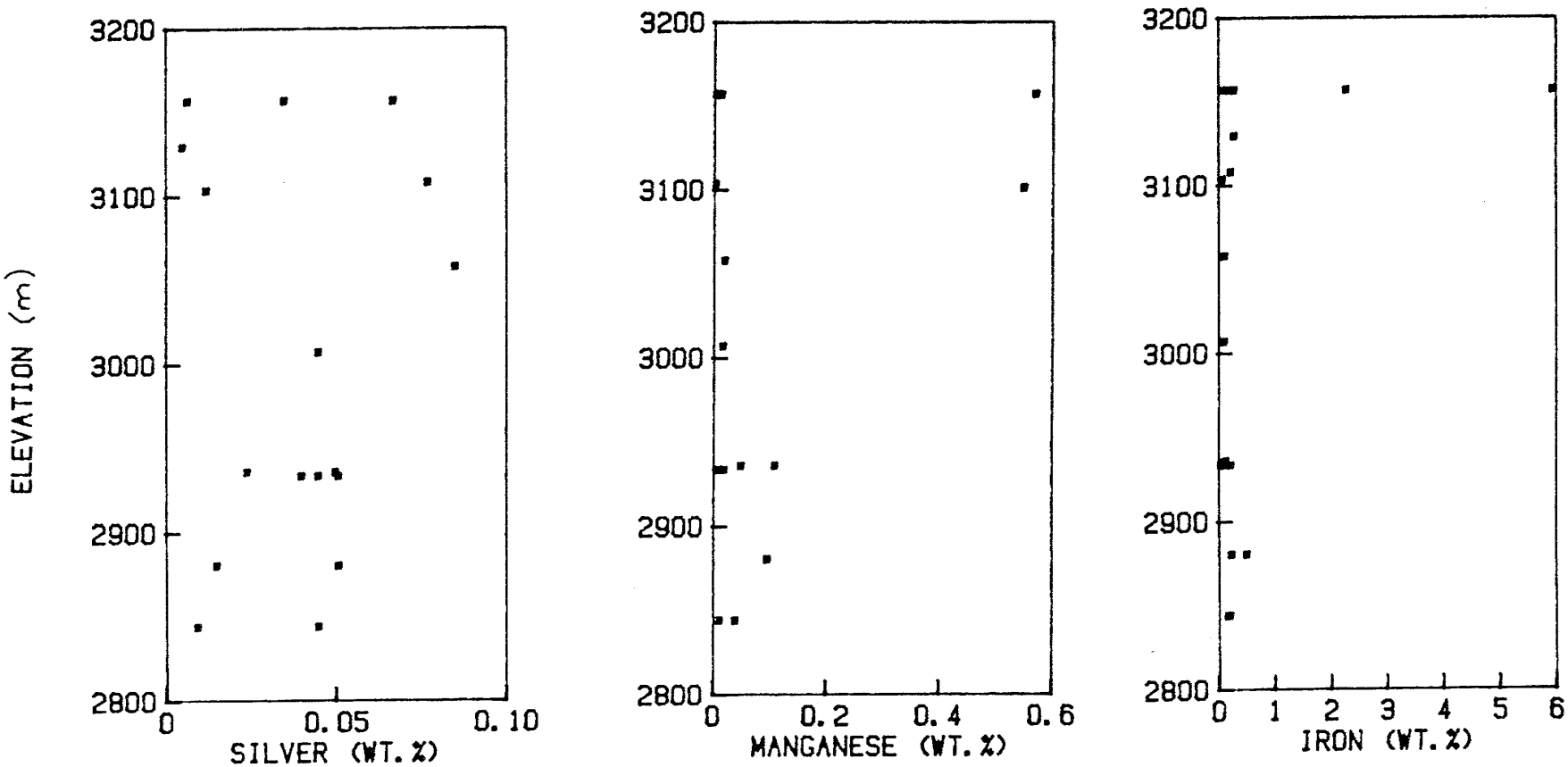
ELEVATION (m)
3200
3100
3000
2900
2800
0
0.05
0.10
SILVER (WT. %)
3200
3100
3000
2900
2800
0
0.2
0.4
0.6
MANGANESE (WT. %)
3200
3100
3000
2900
2800
0
1
2
3
4
5
6
IRON (WT. %)

fluid inclusion analyses were performed on a limited number of samples in order to verify whether the samples studied confirmed the temperature and salinity trends reported. Samples were analyzed from the same range in elevations as that used in the earlier study. Homogenization temperatures were determined for 265 primary and pseudo-secondary inclusions, with freezing temperatures analyzed for 82 of the most readily observable inclusions. The results of this study are consistent with those determined by Robinson and Norman (fig. 8), with average homogenization temperatures within +/-10^{o}C of those from the earlier study, and calculated wt. % NaCl within +/- 1.0 wt. %. This degree of correlation was quite surprising, considering the complexity of mineralization within the vein system, and suggests that the overall pattern of mineralization is regular, despite its complexity in detail. Both sets of results were combined for purposes of geochemical calculation.

Figure 8. Comparison of the results of fluid inclusion analyses from this study and from Robinson and Norman (1984).

a) Homogenization temperatures.

b) Freezing temperatures and equivalent weight percent NaCl.

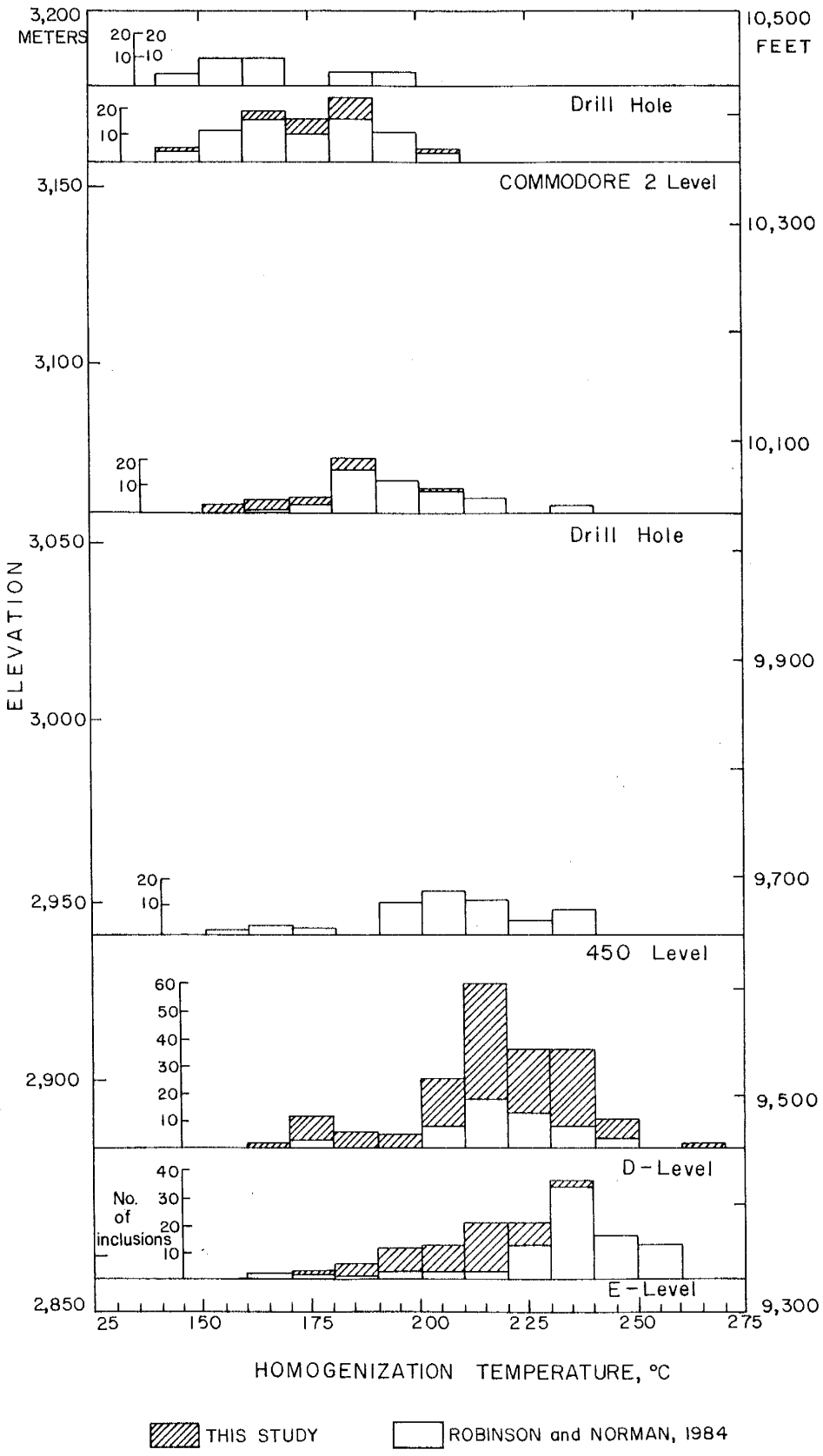
3,200
METERS
10,500
FEET
Drill Hole
COMMODORE 2 Level
3,150
10,300
3,100
10,100
Drill Hole
3,050
9,900
ELEVATION
3,000
2,950
9,700
450 Level
2,900
9,500
D-Level
No. of inclusions
E-Level
2,850
9,300
25
150
175
200
225
250
275
HOMOGENIZATION TEMPERATURE, °C
THIS STUDY
ROBINSON and NORMAN, 1984

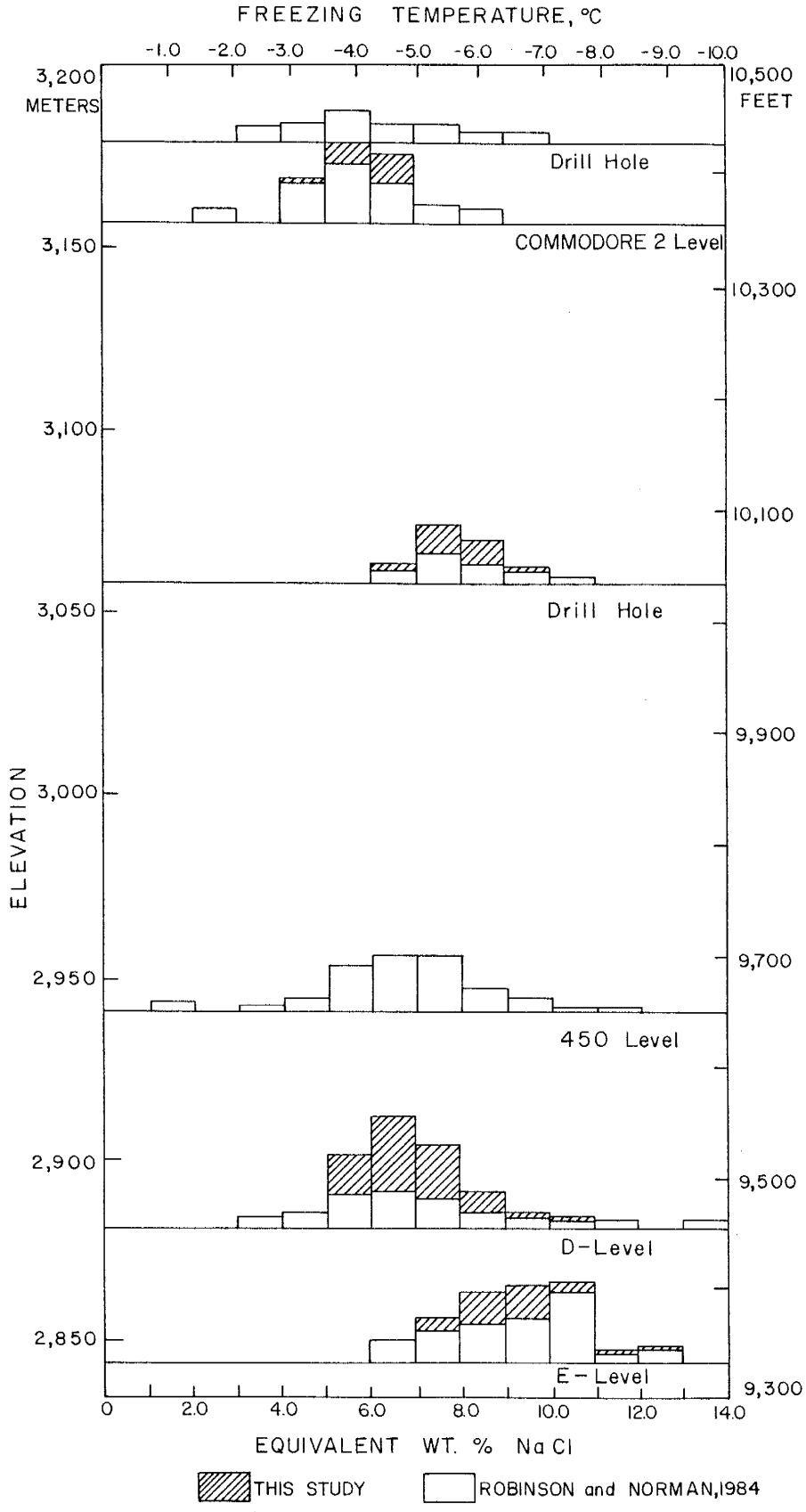
FREEZING TEMPERATURE, °C
-1.0
-2.0
-3.0
-4.0
-5.0
-6.0
-7.0
-8.0
-9.0
-10.0
3,200 METERS
10,500 FEET
Drill Hole
COMMODORE 2 Level
3,150
10,300
3,100
10,100
Drill Hole
3,050
9,900
3,000
ELEVATION
2,950
9,700
450 Level
2,900
9,500
D-Level
2,850
E-Level
9,300
0
2.0
4.0
6.0
8.0
10.0
12.0
14.0
EQUIVALENT WT. % NaCl
THIS STUDY
ROBINSON and NORMAN, 1984

INTERPRETATION

Cyclicity

One observed characteristic of the vein system is the fine layering of vein mineralization. These layers are obviously temporally distinct, yet sulfide grains within different layers exhibit the same sequence of replacement. This implies that either the physicochemical conditions of the depositing fluids were cyclically varying in a regular manner, or that replacement reactions occurred simultaneously within all of the mineralized layers.

The latter possibility is rejected because in most instances the early-formed mineral grains are completely surrounded by quartz, and therefore should have been chemically isolated from later solutions. While there is evidence that some mineral grains were in contact with later mineralizing solutions via fractures in the quartz surrounding the grain (fig. 9), this is of such rare occurrence that it could not have been the cause of replacements observed in most sulfide grains. Instead, the repeated layers of mineralization with identical replacement textures and mineralogy indicate that the replacement was repeated many times in response to cyclical variations in the physicochemical nature of the ore solutions.

Figure 9. Photomicrograph illustrating the mechanism of sulfide replacement due to ore fluid access via microfractures. The microfracture shown has been filled with acanthite (gray), and replacement of the larger galena grain (white) by acanthite has begun at the point of contact between the fracture and the grain. The sulfides are hosted within crystalline vein quartz. Sample 5024B, 50x.

The nature of the replacement reactions observed may be used to determine specifically which parameters were varying. Reactions for the observed replacements are, excluding the reactions involving the sulfosalts for which no thermodynamic data are available, are:

1) $ZnS + Pb^{2+} = PbS + Zn^{2+}$

2) $ZnS + Cu^{+} + Fe^{2+} + H^{+} + 1/4O_2 = CuFeS_2 + 2Zn^{2+} + 1/2H_2O$

3) $ZnS + 2Ag^{+} = Ag_2S + Zn^{2+}$

4) $ZnS + Cu^{+} + H^{+} + 1/4O_2 = CuS + Zn^{2+} + 1/2H_2O$

5) $2FeS_2 + Cu^{+} + H^{+} + 1/4O_2 = CuFeS_2 + Fe^{2+} + S_2 + 1/2H_2O$

6) $2PbS + Cu^{+} + Fe^{2+} + H^{+} + 1/4O_2 = CuFeS_2 + 2Pb^{2+} + 1/2H_2O$

7) $PbS + 2Ag^{+} = Ag_2S + Pb^{2+}$

8) $PbS + Cu^{+} + H^{+} + 1/4O_2 = CuS + Pb^{2+} + 1/2H_2O$

9) $CuFeS_2 + 4Ag^{+} = 2Ag_2S + Cu^{2+} + Fe^{2+}$

10) $CuFeS_2 + Cu^{+} + H^{+} + 1/4O_2 = 2CuS + Fe^{2+} + 1/2H_2O$

11) $Ag_2S + Cu^{+} + H^{+} + 1/4O_2 = CuS + 2Ag^{+} + 1/2H_2O$

and the general reaction:

12) metallic sulfides + Fe^{2+} + O_2 = hematite + metallic ions + S_2

Factors controlling the direction of these reactions include pH, f_{O_2}, temperature, pressure, and the concentrations of metal ions. Several of these parameters, however, probably exerted little control

over the sequence of replacement. Since the effect of pressure on the equilibrium constants for these reactions is negligible below 300°C (Bowers et al., 1985), it is not considered an important parameter. Further, any occurrence of drastic pressure fluctuations during mineralization in the Amethyst vein system is unlikely, considering the open, shallow nature of the vein system, and the absence of explosive breccias in vein material.

Equilibrium constants for reactions 1-4 and 6-10 are strongly dependent on temperature (fig. 10), with that for reaction 5 only slightly dependent. This temperature dependency is such that all replacement reactions, except reaction 5, could have been effected by a change in equilibrium conditions resulting from cooling a fluid without drastically changing the ratios of metal ions in solution. The data in Robinson and Norman (1984) indicate that the ore solutions were in fact quickly cooled in the Amethyst vein system. This conclusion is supported by the fine-grained nature of vein and sulfide minerals at any given locale, which suggests high nucleation rates, generally indicating rapid cooling.

The oxidation-reduction reactions are all dependent upon pH, but the three reactions involving only galena, sphalerite, and acanthite are dependent only upon metal

Figure 10. Plots of metal ion activity ratios vs. temperature for the sulfide replacement reactions observed within the southern Amethyst vein system. Activity ratios are determined from reaction constants calculated from data in Helgeson (1969) and Bowers et al. (1984). Where necessary for calculation, pH was assumed to be equal to 5, log f_{O_2} was assumed to be -35, and log m_{H_2S} was assumed to be -3, based on observed mineralogic and textural characteristics of the vein system (appendix A), and on values calculated in Barton et al. (1977). These values constrain the value of f_{S_2} through the reaction:

$$2H_2S + O_2 = S_2 + 2H_2O$$

to be -1.01, -5.95, and -10.40 at 150°C, 200°C, and 250°C, respectively. Abbreviations used are: GAL, galena; SPH, sphalerite; PY, pyrite; CPY, chalcopyrite; ACA, acanthite; and COV, covellite.

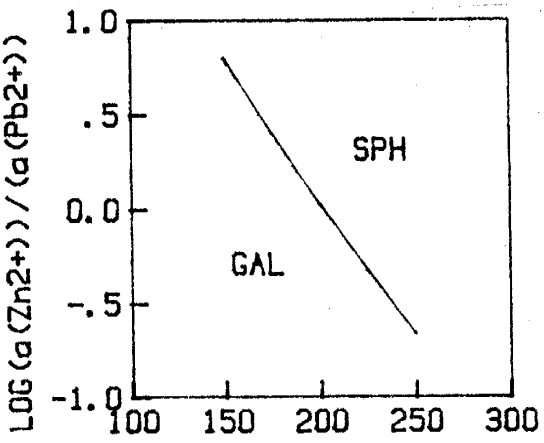
LOG (a (Zn2+)) / (a (Pb2+))
1.0
.5
0.0
-.5
-1.0
100
150
200
250
300
SPH
GAL

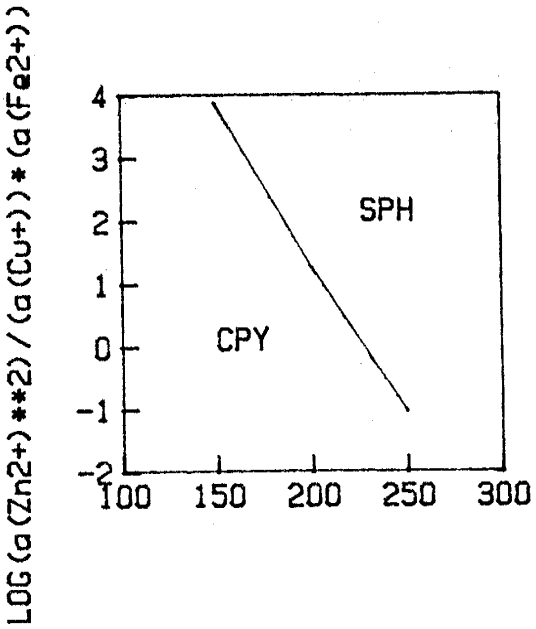
LOG (a (Zn2+) **2) / (a (Cu+)) * (a (Fe2+))
4
3
2
1
0
-1
-2
100
150
200
250
300
SPH
CPY

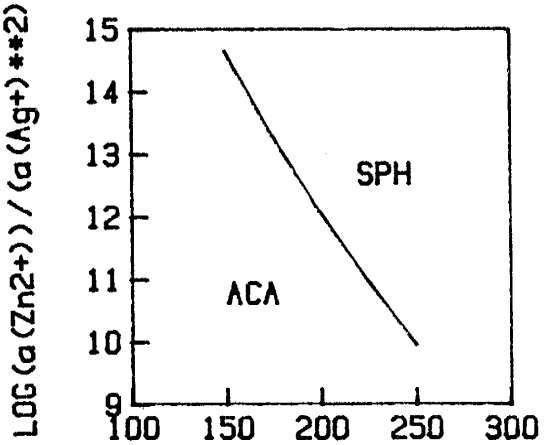
LOG (a (Zn2+)) / (a (Ag+) **2)
15
14
13
12
11
10
9
100
150
200
250
300
SPH
ACA

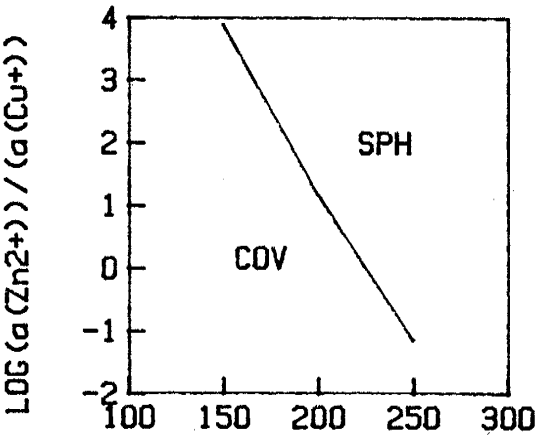
LOG (a (Zn2+)) / (a (Cu+))
4
3
2
1
0
-1
-2
100
150
200
250
300
SPH
COV

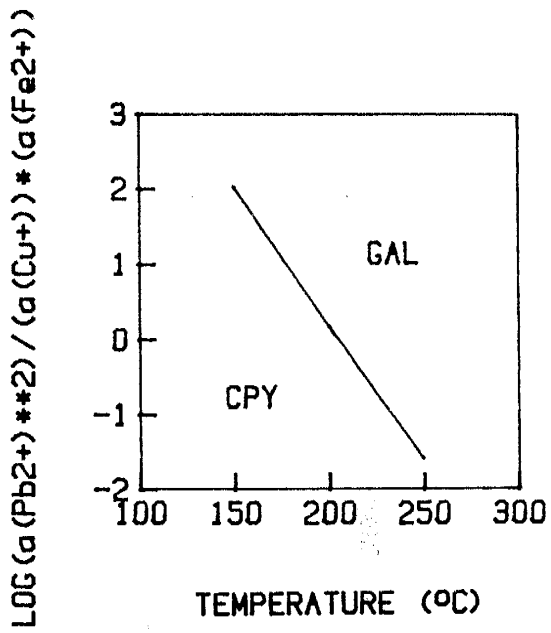
LOG (a (Pb2+) **2) / (a (Cu+)) * (a (Fe2+))
3
2
1
0
-1
-2
100
150
200
250
300
GAL
CPY
TEMPERATURE (°C)

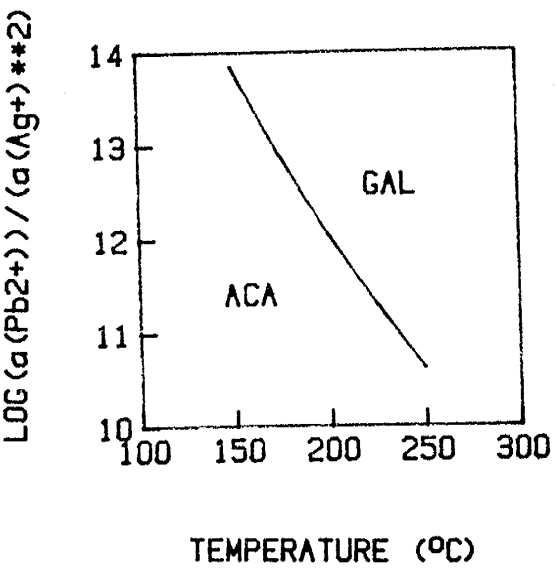
LOG (a (Pb2+)) / (a (Ag+) **2)
14
13
12
11
10
100
150
200
250
300
GAL
ACA
TEMPERATURE (°C)

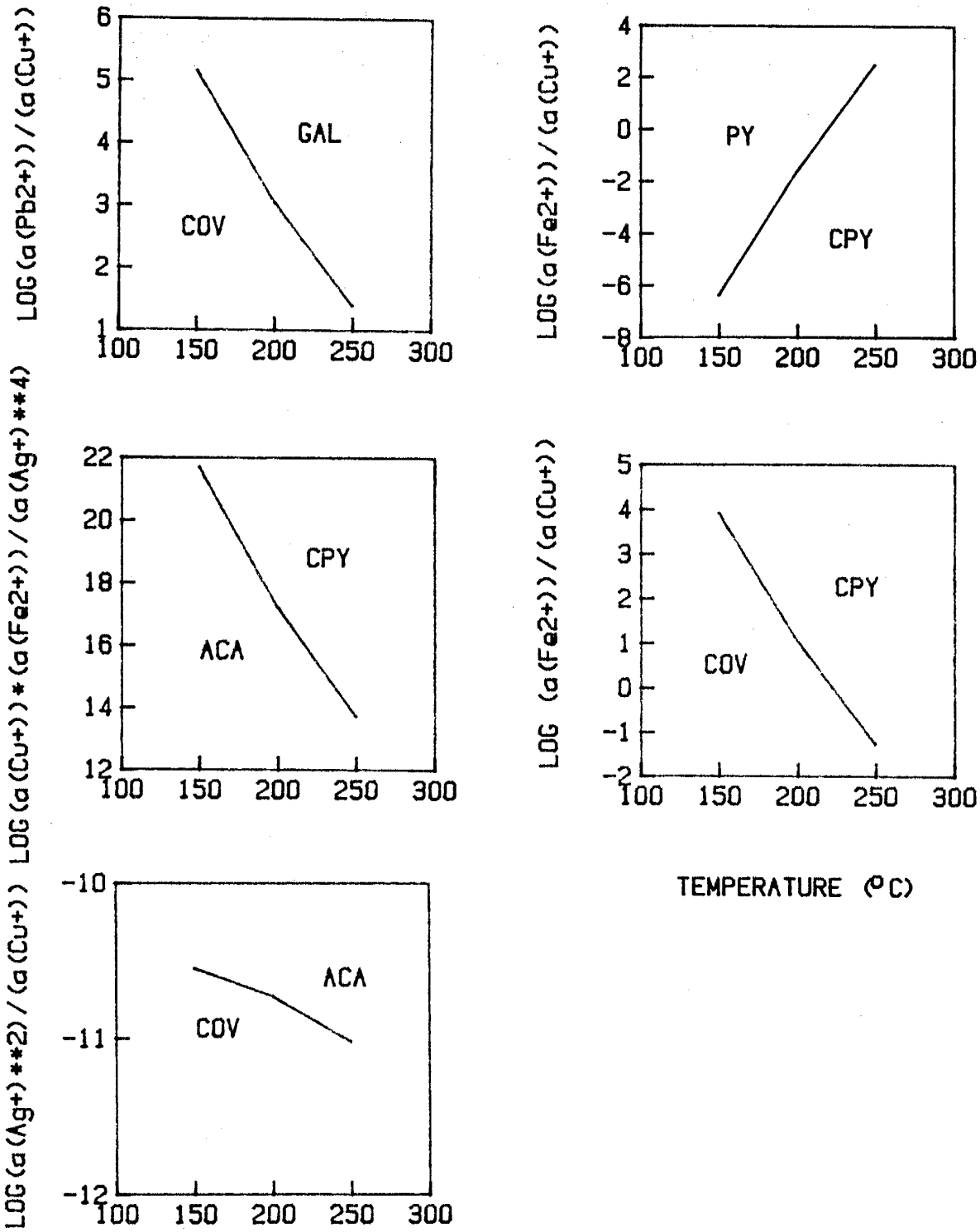
LOG (a(Pb2+)) / (a(Cu+))
6
5
4
3
2
1
GAL
COV
100
150
200
250
300
LOG (a(Fe2+)) / (a(Cu+))
4
2
0
-2
-4
-6
-8
PY
CPY
LOG (a(Cu+)) * (a(Fe2+)) / (a(Ag+) **4)
22
20
18
16
14
12
CPY
ACA
LOG (a(Fe2+)) / (a(Cu+))
5
4
3
2
1
0
-1
-2
CPY
COV
LOG (a(Ag+) **2) / (a(Cu+))
-10
-11
-12
ACA
COV
TEMPERATURE (°C)
TEMPERATURE (°C)

ion ratios and temperature. This would imply that pH was not the principal parameter involved in replacement reactions. Furthermore, fluctuations in pH typically involve either wall-rock reaction or boiling. There is no evidence for either pervasive intense alteration in the country rock or for boiling, suggesting an absence of pH changes.

All the reactions are, of course, dependent upon the concentration of metal ions in solution. To be solely responsible for the replacement sequence observed, however, specific metals would have to vary in solution in a very regular manner. For example, zinc must predominate initially to precipitate sphalerite, followed by a predominance of lead to replace sphalerite with galena, etc. In addition, given the cyclical nature of vein deposition, this specific variance would have to have been repeated many times, once for each cycle of replacement. This is considered unlikely.

Increasing f_{O_2} values could have been responsible for replacement reactions 2, 4, 5, 6, 8, 10, 11, and 12. In addition, the replacement of acanthite by covellite (reaction 11), which is only slightly affected by a decrease in solution temperature, proceeds with an increase in f_{O_2} (see reaction 11), and is in fact stongly f_{O_2}-dependent (fig. 11). This is also true for the replacement of pyrite by chalcopyrite by pyrite

Figure 11. Plots of metal ion activity ratios vs. f_{O_2} for the replacement of acanthite by covellite. The activity ratio was determined from reaction constants calculated from data in Helgesson (1969) and Bowers et al. (1984). A value for pH of 5 was assumed, based on the value calculated by Barton et al. (1977).

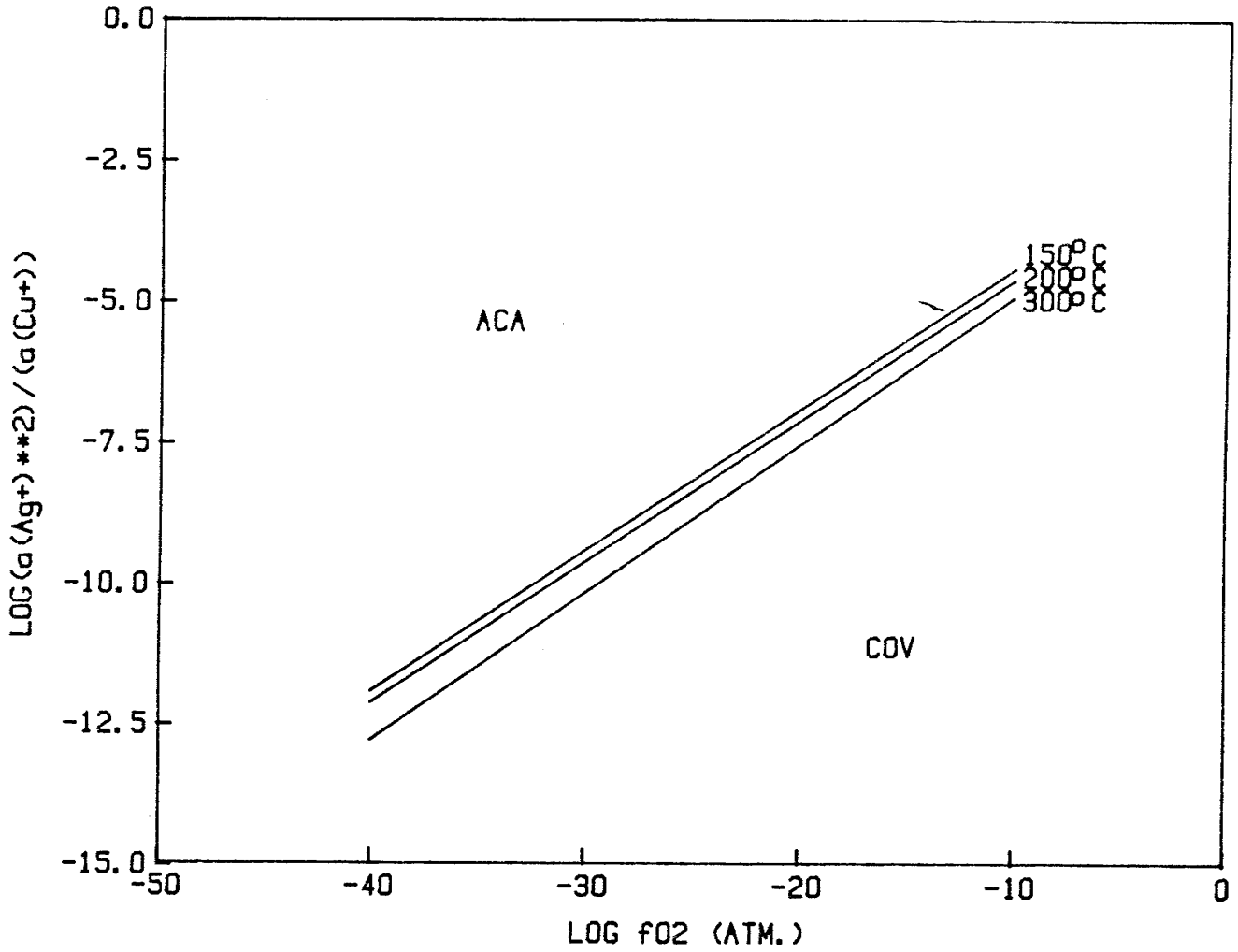
0.0
-2.5
-5.0
-7.5
-10.0
-12.5
-15.0
LOG(a(Ag+)**2)/(a(Cu+))
-50
-40
-30
-20
-10
0
LOG fO2 (ATM.)
ACA
COV
150° C
200° C
300° C

(reaction 5), which would not have resulted from a temperature decrease, but would have resulted from an increase in f_{O_2}. The replacement of sulfides by hematite and the hematite coatings observed at many boundaries between layers of vein mineralization are good evidence for an increase in f_{O_2} having occurred during each replacement cycle. The occurrence of manganese carbonates only at low elevations within the system, with manganese oxides present at higher levels suggest that f_{O_2} levels also increased with elevation.

On balance, there is ample physical and chemical evidence that changes in two parameters controlled the sequence of replacement in the southern Amethyst vein system. These are a decrease in mineralizing fluid temperature and an increase in f_{O_2}. Other parameters, such as fluctuations in pH, pressure, and the concentration of dissolved metallic species, are considered far less likely to have resulted in the replacements observed.

This conclusion may be significant on a scope broader than that of the study area. The replacement sequence recorded is specifically associated with a temperature decrease. Therefore, the presence of this same sequence in other epithermal deposits could serve as a strong positive indicator of rapid cooling of ore solutions, either due to mixing or to some other

mechanism. Such knowledge could prove an invaluable addition to that obtained by commonly-used methods of ore genetic study, such as fluid inclusion analysis.

During the period when detailed studies of sulfide intergrowth textures were commonly performed (primarily the 1930's and 1940's), several examples of deposits which exhibit replacement sequences similar to those here presented are reported (e.g., Lindgren, 1935; Bastin, 1941; Goodspeed, 1936; Bastin, 1948). In fact, a sequence of sulfide mineralization almost identical to that determined in this study was considered characteristic for epithermal deposits by Lindgren (1933). These facts suggest that studies of this type may be useful on a wider scale than that they presently enjoy.

Vertical Variations in Mineralization

Although lateral control was less extensive than vertical control in sampling, it is still apparent that lateral variations (variations along the same elevation) in mineralogy, fluid inclusions, and geochemistry are minor compared to those observed with changes in elevation. For this reason, elevation is assumed to be the controlling spatial variable within the southern Amethyst vein system.

The occurrence of silver sulfides predominantly at upper elevations within the vein system, and the predominance of base metal sulfides at lower mine elevations, can be readily explained by consideration of mineral solubilities and metal complexation behaviour. Based on fluid inclusion evidence from Robinson and Norman (1984) and this study, the ore solutions are assumed to progress through three stages of temperature and salinity, from a temperature of 250^{o}C and a salinity of 9 wt.% (m_{NaCl}=1.54) at the lowest elevations in the vein system to an intermediate stage, with a temperature of 200^{o}C and a salinity of 7 wt.% (m_{NaCl}=1.20), to a temperature of 150^{o}C and a salinity of 5 wt.% (m_{NaCl}=0.86) at the highest mine elevations. These values represent the two approximate end members and an intermediate value for the continuum of fluid temperatures and salinities suggested by fluid inclusion data. The intermediate value was chosen based on the fact that elevations with fluid inclusion temperatures and salinities of appproximately 200^{o}C and 7 equivalent wt.% NaCl are the lowest at which silver mineralization is observed to be abundant. Metals in solution are assumed to exist only as chlorocomplexes or the simple (uncomplexed) ion, an assumption reasonable in a solution with salinities in the 5 to 10 weight percent NaCl range (Weissberg et al., 1979). The amounts of dissolved Pb and Ag in equilibrium with galena and

acanthite at the base of the Southern Amethyst vein system were calculated.

The high lead values (fig. 7) and occurrence of galena indicate that during intervals of sulfide deposition, solutions were saturated with respect to lead sulfide. Should this have been true for silver sulfide as well (since the two sulfides have similar solubilities (fig. 12)), silver values roughly equivalent to those of lead in the lower part of the vein system would have resulted. Since this is not the case, Ag concentrations in solution must have been substantially lower than those of Pb.

The ratio of these metals in solution may be estimated using the equilibrium values for the galena-acanthite replacement reaction. At 200^{o}C (the highest temperature at which abundant silver mineralization is observed), the equilibrium ratio for $aPb^{2+}/aAg^{+}**2$ is approximately 10E12 (fig. 10). At elevated temperatures and salinities only a very small percentage of the dissolved metals exists as the simple ionic form, the remainder being present as various chlorocomplexes (fig. 12). Calculations based on these data yield a molar Pb/Ag ratio of 11, indicating that solutions saturated with respect to lead (1.6 ppm Pb) should have an Ag concentration of 0.27 ppm. At this silver concentration, saturation with respect to silver

Figure 12. Solubility behaviour of lead and silver at 150°C, 200°C, and 250°C. A pH of 5 and m_{H_2S} of 10^{-3} is assumed, based on the findings of Barton et al. (1977).

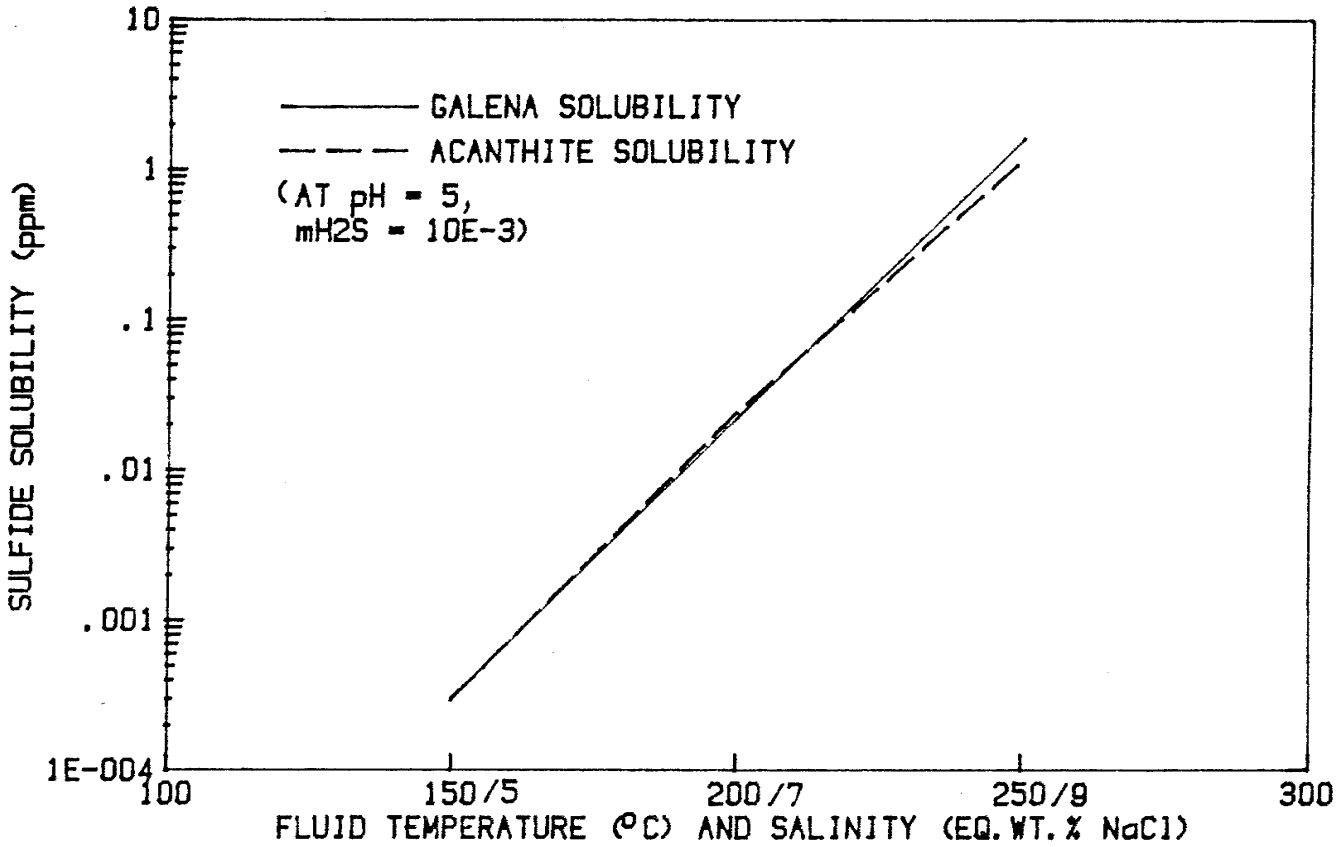
10
1
.1
.01
.001
1E-004
SULFIDE SOLUBILITY (ppm)
GALENA SOLUBILITY
ACANTHITE SOLUBILITY
(AT pH = 5,
mH2S = 10E-3)
100
150/5
200/7
250/9
300
FLUID TEMPERATURE (°C) AND SALINITY (EQ. WT. % NaCl)

sulfide would not be approached until the solutions reached temperatures and salinities found only in the upper part of the system.

Interestly, a Pb/Ag weight ratio of 21 in the mineralizing fluid would suggest that the grade of Ag in the upper levels of the Amethyst vein system should have been about 1/21 of that of lead in the lower part of the vein. Our values of approximately 2.5 % Pb in the lower elevations would suggest that the upper part of the vein system should have about 0.12 % Ag (36 oz. Ag/ton). Historically, vein mineralization has produced grades within the study area of approximately 46 oz. Ag/ton (Robinson and Norman, 1984).

Nature of the Mineralizing System

Since a decrease in temperature and increase in f_{O_2} are indicated to have controlled the replacement, these parameters must also have fluctuated in a cyclical fashion. This requires a temperature decrease and f_{O_2} increase to have occurred as sulfides were precipitated within each band of vein mineralization. Rather than fluctuating the temperature and f_{O_2} repeatedly throughout the entire 375 m vertical section of the vein system, a more probable idea is suggested by the stacked-cell convection model proposed for Creede by Berger and Eimon (1982) (fig. 13). Such a model suggests cool, dilute fluids entering a system from the

Figure 13. Fluid flow within a proposed stacked-cell convection system within the southern Amethyst vein system. The alteration cap shown occurs to the north of the proposed zone of mixing, and is the result of acid leaching related to boiling (Barton et al., 1977).

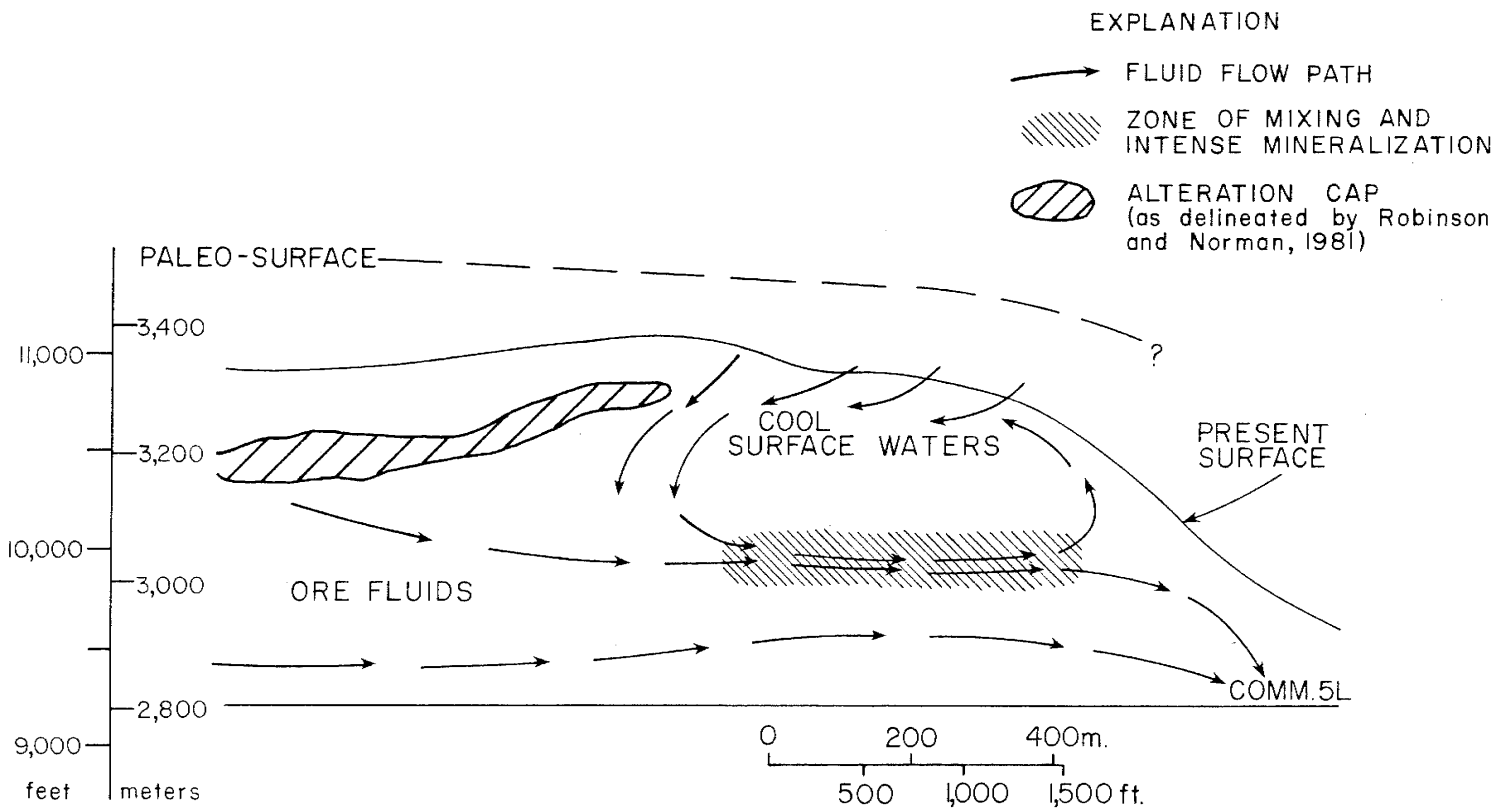
EXPLANATION
FLUID FLOW PATH
ZONE OF MIXING AND INTENSE MINERALIZATION
ALTERATION CAP (as delineated by Robinson and Norman, 1981)
PALEO-SURFACE
?
11,000
3,400
3,200
10,000
3,000
2,800
9,000
feet
meters
COOL SURFACE WATERS
PRESENT SURFACE
ORE FLUIDS
COMM.5L
0
200
400m.
500
1,000
1,500 ft.

surface encounter hotter, more saline solutions rising from below. Separate convection cells are formed by the fluids, one overlying the other with a laterally moving interface between. The mixing of the solutions at the interface between the convection cells would result in the cooling and dilution of the rising metalliferous solutions. As a result, most mineralization occurs along this mixing zone. The vertical position of this interface would reasonably be expected to fluctuate with varying rates of influx for the two solutions.

The Southern Amethyst vein system might have been an ideal candidate for establishing such a system, since the intersection of the Creede formation breccias by the Amethyst vein system would have allowed ready access to surface waters at the top of the vein system. These could have mixed freely with the hot, metalliferous brines entering from the northern end of the vein system, due to the open, interconnecting nature of the mineralized structures. This ease of circulation would have facilitated the development and movement of convection cells. Further, the mingling of the fluids at the interface between cells would explain the evidence of extensive fluid mixing observed by Robinson and Norman (1984).

Assuming that most of the vein mineralization occurred at the interface in a stacked cell system, repeated shifts in vertical position could move the interface back and forth past any point in a vein (fig. 14). This process would produce a finely layered style of vein mineralization, with each layer deposited as the interface passes point of deposition. Temporal changes in solution character would account for variations in vein mineralogy between layers.

Most importantly, since the metalliferous solutions were mixing with cooler, more oxygenated surface fluids, sulfides deposited at the interface would have been subjected to both a temperature decrease and an f_{O_2} increase. This would have been repeated each time the mixing zone deposited another layer of vein mineralization, resulting in the observed series of layers, each containing sulfides with the same sequence of replacement.

Disseminated minerals display only one series of replacements, indicating they were isolated from later solutions in some way. Silicification of the wall rock is common throughout the vein system. If such silicification occurred contemporaneously with the first sequence of mineralization and replacement (which also presumably deposited the disseminated minerals), the disseminated mineralization could have been isolated

Figure 14. Proposed mechanism for producing a finely-layered style of vein mineralization due to fluctuations in the elevation of the interface between convection cells.

a) Interface at approximately 3100 m elevation. Major deposition of vein minerals occurs at this elevation (layer 1), due to the effects of cooling and dilution of ore fluids due to mixing.

b) Interface rises in elevation to above 3200 m elevation. Only relatively minor deposition (layer 2) occurs at 3100 m elevation, due to the absence of fluid mixing.

c) Interface descends again past 3100 m elevation. Major deposition (layer 3) resumes with the return of the zone of mixing to this level.

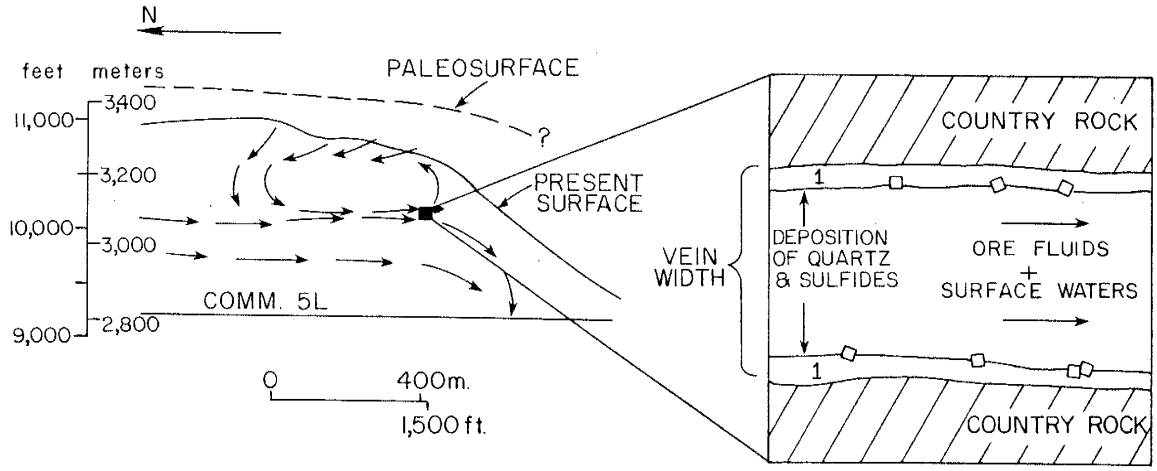
N
feet
meters
PALEOSURFACE
?
11,000
3,400
3,200
10,000
3,000
9,000
2,800
PRESENT
SURFACE
COMM. 5L
0
400m.
1,500 ft.
VEIN
WIDTH
COUNTRY ROCK
1
DEPOSITION
OF QUARTZ
& SULFIDES
ORE FLUIDS
+
SURFACE WATERS
1
COUNTRY ROCK

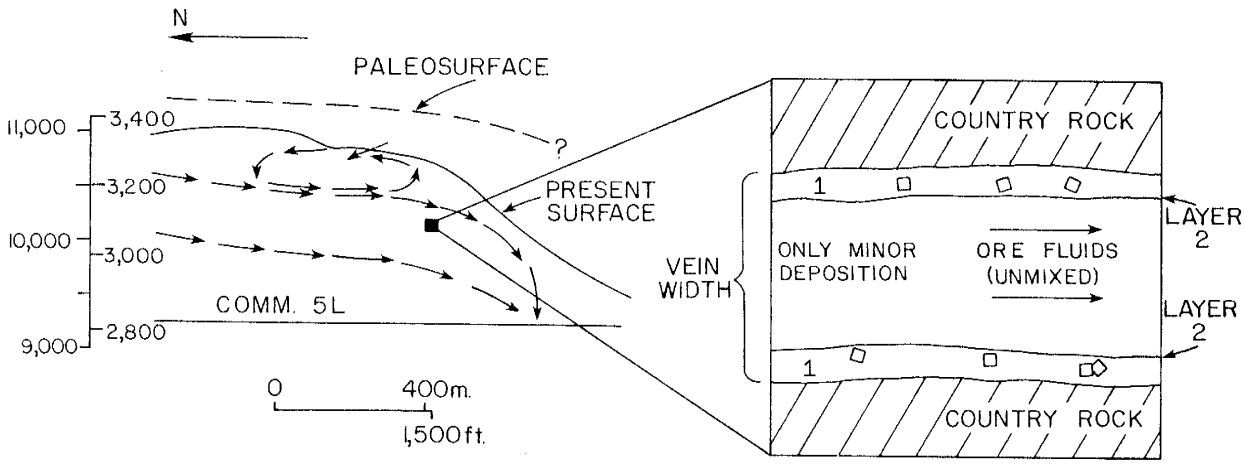
N
PALEOSURFACE
?
11,000
3,400
3,200
10,000
3,000
9,000
2,800
PRESENT
SURFACE
COMM. 5L
0
400m.
1,500 ft.
VEIN
WIDTH
COUNTRY ROCK
1
ONLY MINOR
DEPOSITION
ORE FLUIDS
(UNMIXED)
LAYER
2
LAYER
2
1
COUNTRY ROCK

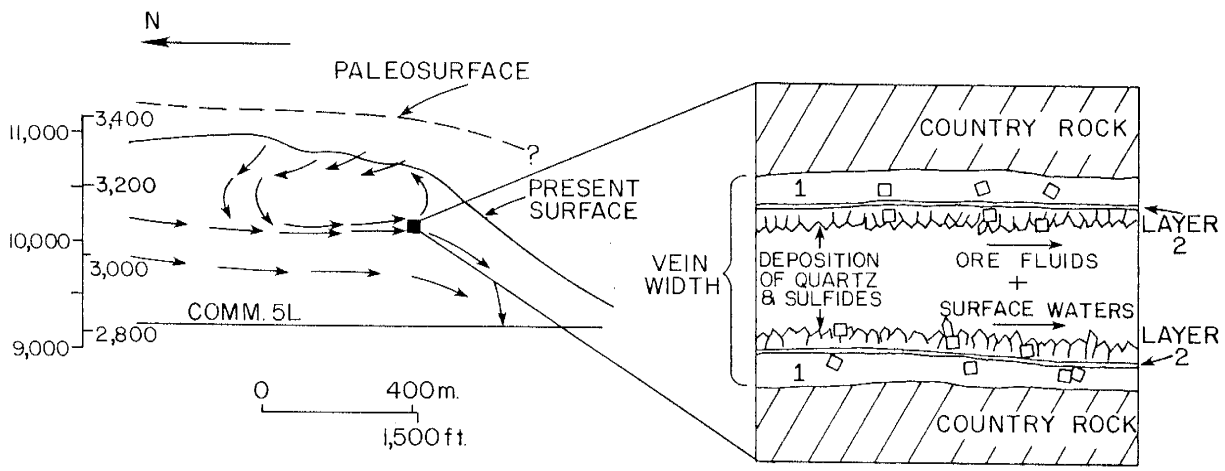
N
PALEOSURFACE
?
11,000
3,400
3,200
10,000
3,000
9,000
2,800
PRESENT
SURFACE
COMM. 5L
0
400m.
1,500 ft.
VEIN
WIDTH
COUNTRY ROCK
1
LAYER
2
DEPOSITION
OF QUARTZ
& SULFIDES
ORE FLUIDS
+
SURFACE WATERS
LAYER
2
1
COUNTRY ROCK

from later solutions. This would have precluded overprinting of later replacements on the initial sequence. Such "sealing" of the disseminated mineralization is suggested by Giudice (1980) to have occurred.

The hematite banding observed between some layers within veins could have been deposited by deeper movement of the interface and the resultant contact with the higher f_{O_2} concentrations above the mixing zone. Movement of the interface upwards would have resulted in an increase in temperature. This should not have caused etching of vein quartz, however, since the hotter solutions would be expected to be nearly or super-saturated with respect to silica. No etching or pitting of quartz was observed.

Although the relatively simple pattern of fluid inclusion temperatures and salinities is not obviously explicable by stacked cell convection, it could have occurred within the general framework of the proposed system. Any of several factors could have contributed to this type of data pattern; these include the presence of a broad, diffuse interface (zone of mixing) rather than a sharply defined one, the action of minor mixing not controlled by the interface, or the presence of multiple interfaces, rather than a single one. Overall, this is simply an indication that the proposed

stacked-cell system may be an oversimplification, and that the nature of mixing within the southern Amethyst vein system was quite complex.

CONCLUSIONS

Fault- and fracture-hosted mineralization within the Southern Amethyst vein system is typically fine-grained, finely-laminated (within veins), and high in silver grades. Replacement textures in sulfide intergrowths are ubiquitous, and replacement occurs in a consistent sequence, even within several temporally distinct layers within veins. Geochemical calculations based on this replacement sequence indicate that a ore solutions were quickly and cyclically cooled. Fluid inclusion data suggest that ore solutions were progressively mixed as they circulated through the vein system.

The style of mineralization and high silver grades observed are believed to be due to the presence of a mixing system within the southern Amethyst vein system. Upon entering the the southern extent of the Amethyst vein system, ore solutions encountered descending, cool, oxidizing, surficial waters. A system of stacked convection cells was established, with the cooler solutions circulating within a convection cell overlying that in which the hotter, metalliferous fluids circulated. Between the two cells was a zone of mixing, where strong cooling and dilution of the ore solutions by the surface fluids resulted in rapid, intense mineralization. This cooling, in addition to the

increase in f_{O_2} which accompanied it, also resulted in a series of replacement reactions involving the sulfides present. Movement of the mixing zone due to shifts in convection cell position resulted in a finely banded style of vein mineralization, as this area of high precipitation swept repeatedly across vein surfaces. This also produced a cyclical pattern of replacement in the sulfides within these layers, since sulfides within different layers all experienced the same sequence of replacement.

The ore solutions entering the southern Amethyst vein system were undersaturated with respect to silver sulfide, and had a molar Pb/Ag ratio of approximately 11. As a result, saturation and resultant precipitation of acanthite did not occur until after significant cooling and dilution of the ore solutions, which process confined the bulk of silver mineralization to the upper levels of the vein system.

APPENDIX A

Geochemical Calculations

The reactions chosen to model the replacement sequence observed in the southern Amethyst vein system were the simplest which accurately conformed to actual geochemical conditions. This criterion was easily applied to reactions involving only lead, zinc, and silver, since these metals exist only as univalent ions in solution, and since these reactions have no pH or f_{O_2} dependency.

Reactions involving copper and iron, however, are more complex. These metals are polyvalent, and the reactions in which they occur are typically both pH- and f_{O_2}-dependent. In these cases, the way in which the reaction was written was dictated primarily by the oxidation state chosen for copper and/or iron. This choice was made on the basis of which oxidation state would be predominant under the general temperature and oxidation conditions expected to have existed in the vein system.

Calculation of Cu^{+}/Cu^{2+} ratios was based on the reaction constants calculated by Helgeson (1969) for the oxidation of the cuprous ion to the cupric one. As illustrated in figure 15, Cu^{+} would be stongly predominant under hydrothermal conditions, a conclusion supported by Barnes (1979). As a result, in reactions

Figure 15. Plot of log Cu^{2+}/Cu^{+} activity ratio vs. log f_{O_2} for the temperatures observed in the southern Amethyst vein system.

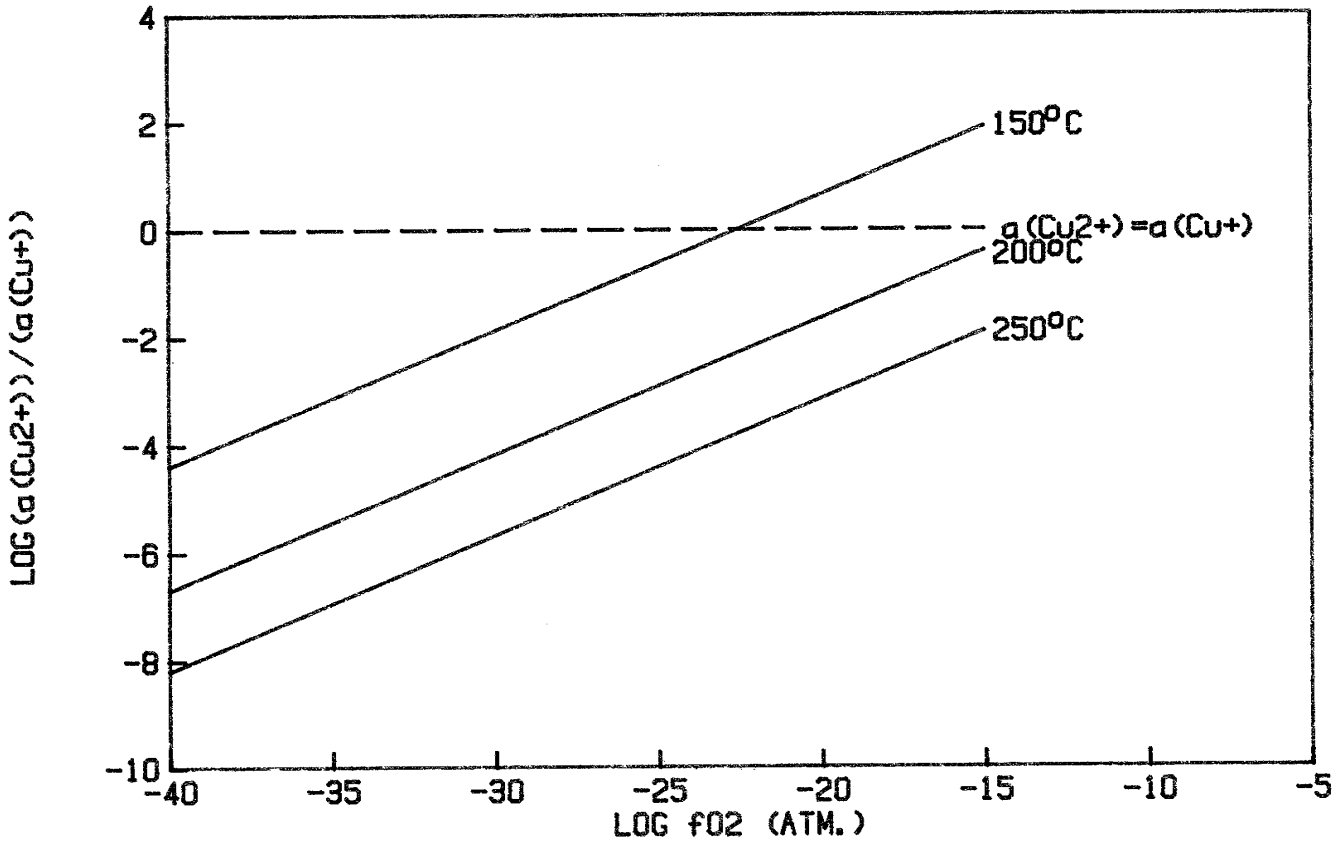
4
2
0
-2
-4
-6
-8
-10
-40
-35
-30
-25
-20
-15
-10
-5
LOG (a (Cu2+)) / (a (Cu+))
LOG fO2 (ATM.)
150°C
a (Cu2+) =a (Cu+)
200°C
250°C

where copper is a reactant, Cu^{+} was used. This predominance would not, of course, affect reactions where copper was a product. Cu^{2+} can appear in the right side of these reactions under this line of reasoning, and, in fact, does so in reaction 11. Under the same rationale, Fe^{2+}, rather than Fe^{3+}, is used as a reactant in reactions involving iron, rather than Fe^{3+}.

Once reactions were written, their dependency on temperature was calculated. First, reaction constants were determined for each reaction based on equilibrium data in Helgeson (1969) and Bowers et al. (1984) for dissociation or hydrolysis of the various sulfides and other species involved. These reactions and their reaction constants were summed until the final reaction format was attained.

Example:

For the replacement of acanthite by covellite:

Reaction	log K(T)		
	150°C	200°C	250°C
$Ag_2 = 2Ag^{+} + S^{2-}$	-35.45	-31.71	-28.74
$Cu^{2+} + S^{2-} = CuS$	28.21	26.28	24.73
$Cu^{+} + 1/4O_2 + H^{+} = Cu^{2+} + 1/2H_2O$	10.34	8.35	6.64
$Ag_2 + Cu^{+} + 1/4O_2 + H^{+} = 2Ag^{+} + CuS + 1/2H_2O$	3.10	2.92	2.63

Since $K(T) = a(Ag^+)^{**}2/a(Cu^+)*((a(O_2))^{**}1/4)*a(H^+)$,
log K(T) may be expressed as :

$$\log K(T) = \log(a(Ag^+)^{**}2/a(Cu^+)) + pH - 1/4(\log(f_{O_2})).$$

Simple manipulation of this equation yields:

$$\log(a(Ag^+)^{**}2/a(Cu^+)) = \log K(T) + 1/4(\log(f_{O_2})) + pH.$$

Assuming a pH of 5 and an $\log(f_{O_2})$ of -34.6, this equation yields values for the ratio of the metal activities of -10.55, -10.73, and -11.02 for temperatures of 150°C, 200°C, and 250°C, respectively.

In the case of the non-redox reactions, due to the absence of pH or f_{O_2} dependency, the determined reaction constant is also equal to the ratio of the two metal ions involved in replacement. For example, for the replacement of sphalerite by galena, the reaction constant at each temperature is also the ratio of the activity of Zn^{2+} to that of Pb^{2+} ($K = a(Zn^{2+})/a(Pb^{2+})$, therefore $\log K = \log((a(Zn^{2+}))/(a(Pb^{2+})))$.

For the redox reactions, the process is more complex. Both a pH value and an f_{O_2} must be chosen to calculate the ratios of various metal ions from reaction constants. Values for these parameters were estimated on several bases. Barton et al. (1977) estimate a pH of slightly greater than 5 for fluids within the OH-vein, based on mineral assemblages. Since no drastic pH changes are indicated within the Amethyst vein system, a value of 5 was chosen for purposes of

calculation. The oxidation of galena and sphalerite was rarely observed; this constrains the log f_{O_2} values to less than approximately -30. This value is supported again by Barton et al., who estimate an log f_{O_2} of approximately 35 for the OH-vein. This value was used for geochemical calculations for the southern Amethyst vein system.

Complexation was calculated based upon stepwise and cumulative complexation constants in Seward (1976, 1984), combined where necessary with reaction data from Helgesson (1969). Solubility of silver and lead sulfides were calculated from data from the same sources. The results of calculations are summarized in Table 1. Calculations were performed using a modification of the PbS program developed by R.W. Henley, and described in Henley et al. (1984).

Table 1. Chloro-complexation of Lead and Silver and the Solubility of Lead and Silver Sulfides as a Function of Idealized Ore Fluid Temperatures and Salinities. Values of 5 for pH and of 10^{-3} for m_{H_2S} are assumed, based on data from Barton et al. (1972). Saturation concentrations for Pb and Ag are based on saturation with galena and acanthite.

Mine Level (elevation)	Ore Fluid Temperature and Salinity	Complexation	Sulfide Saturation
Commodore 2 (3156.8 m)	150°C 5 eq.wt.% NaCl (0.857 m)	Total Pb = 2.1409% Pb^{2+} 21.9641% $PbCl^{+}$ 55.2636% $PbCl_3^{-}$ 20.6314% $PbCl^{3-}$	$m_{Pb_{sat}} = 10^{-8.840}$
		Total Ag = 0.0244% Ag^{+} 3.1895% $AgCl$ 96.7891% $AgCl_2^{-}$	$m_{Ag_{sat}} = 10^{-8.567}$
Sublevel C (2904 m)	200°C 7 eq.wt.% NaCl (1.20 m)	Total Pb = 0.3610% Pb^{2+} 9.0712% $PbCl^{+}$ 52.4410% $PbCl_2^{2-}$ 38.1268% $PbCl_3^{-}$	$m_{Pb_{sat}} = 10^{-6.976}$
		Total Ag = 0.0137% Ag^{+} 1.7408% $AgCl$ 98.2454% $AgCl_2^{-}$	$m_{Ag_{sat}} = 10^{-6.654}$
Sublevel E (2844 m)	250°C 9 eq.wt.% NaCl (1.54 m)	Total Pb = 0.0428% Pb^{2+} 3.6272% $PbCl^{+}$ 37.2779% $PbCl_2^{2-}$ 59.4121% $PbCl_3^{-}$	$m_{Pb_{sat}} = 10^{-5.112}$
		Total Ag = 0.0059% Ag^{+} 1.1548% $AgCl$ 98.8393% $AgCl_2^{-}$	$m_{Ag_{sat}} = 10^{-4.963}$

APPENDIX B

Sulfide Intergrowth Textures

The sulfides present displayed a number of intergrowth textures, both with other sulfides and with oxide and gangue minerals. The primary form of mineralization was probably sphalerite with or without pyrite. Sphalerite is quite common, both in terms of abundance of occurrence and of intergrowths with other sulfides. Pyrite is much less abundant, and intergrowths are of rare occurrence. Where the two occur together, rarely occurring incomplete reaction rims of sphalerite around pyrite implies that pyrite may have been the earlier mineral, but the scarcity of these textures precludes any certainty. Complete reaction rims of chalcopyrite around pyrite definitely places pyrite in the earliest part of the sequence.

Sphalerite was most commonly replaced by galena, which was the most abundant sulfide in most samples. A variety of textures were exhibited between these two phases, including simple and mottled intergrowths, caries texture, inclusions, and both complete and incomplete reaction rims. The sphalerite/chalcopyrite replacement reaction produced dominantly simple intergrowth textures and scattered mottled intergrowths, but several occurrences of complete reaction rims indicate a clear temporal relationship. The

sphalerite/covellite reaction occurs more rarely, with simple intergrowths and occasional reaction rims. The sphalerite to acanthite reaction is quite uncommon, and was observed only as inclusions and atoll textures.

Galena was commonly intergrown with chalcopyrite, exhibiting the same range of textures seen between galena and sphalerite, with the exception of caries texture. The galena/covellite reaction was also quite common, with simple and mottled intergrowths most abundant, more rarely occurring examples of complete and incomplete reaction rims, and very rarely occurring (only two examples seen) of pseudo-graphic intergrowths. Galena is frequently replaced by acanthite, exhibiting simple intergrowths and some perfect reaction rims.

Chalcopyrite shows abundant replacement by covellite, with textures dominated by simple intergrowths and incomplete reaction rims. Complete rims do occur, however, and are abundant enough to establish the order of replacement. Chalcopyrite is infrequently replaced by sulfosalts and acanthite. These textures are predominantly simple intergrowths, but rare examples of complete atoll textures were observed.

Acanthite, where present, was replaced by sulfosalts, typically forming reaction rims of variable completeness. When acanthite was replaced by

sulfosalts, both these phases were almost invariably subsequently replaced by covellite. While reaction rims were observed, by far the most common mode of replacement is as covellite needles growing into sulfosalt and acanthite layers.

Sulfosalts are observed only in association with acanthite, typically as part of a replacement rim on galena grains. Tetrahedrite was of very rare occurrence in samples analyzed, and occurs as fine-grained marginal blebs on larger bodies of other sulfosalts. Although inconclusive, this positioning implies the sulfosalts may have preceded the tetrahedrite. Needles of covellite do cross-cut the tetrahedrite, placing it with good certainty between covellite and acanthite, so only the relationship with the undivided sulfosalts is in question.

Covellite was the final sulfide phase present throughout the system. As noted, it exhibits simple, mottled and reaction rims with most base-metal sulfides, but appears as needle-like ingrowths in most precious-metal sulfides and with sulfosalts.

Finally, alabandite is also present, although its position in the paragenetic sequence is unknown. It is generally observed as fine, subequant grains spatially associated with other manganese minerals, especially manganese carbonates.

APPENDIX C

Sample Locations

Table 2. Elevations of samples taken from underground exposures, and depths (along the line of coring) below surface for drill core samples.

Sample Locations

Sample	Type (UG = underground) (DC = drill core)	Mine Level or Drill Hole	Elevation(m) (for UG) Depth(m) (for DC)
5001	UG	Commodore 2	3156.8
5002	UG	Commodore 2	3156.8
5003	UG	Commodore 2	3156.8
5004	UG	Commodore 2	3156.8
5005	UG	Commodore 2	3156.8
5006	UG	Commodore 2	3156.8
5007	UG	Commodore 2	3156.8
5008	UG	Commodore 2	3156.8
5009	UG	Commodore 2	3156.8
5010	UG	Sub-level E	2843.9
5011	UG	Sub-level E	2843.9
5012	UG	Sub-level E	2843.9
5013	UG	Sub-level E	2843.9
5014	UG	Sub-level D	2880.2
5015	UG	Sub-level D	2880.2
5016	UG	Sub-level D	2880.2
5017	UG	Sub-level D	2880.2
5018	UG	Commodore 450	2935.6
5019	UG	Commodore 450	2935.6
5020	UG	Commodore 450	2935.6
5021	UG	Commodore 450	2935.6
5022	UG	Commodore 4	2933.3
5023	UG	Commodore 4	2933.3
5024	UG	Commodore 4	2933.3
5025	DC	CDS 4	215.8
5026	DC	CDS 4	80.8
5027	DC	CDS 4	138.1
5028	DC	CDS 4	154.8
5029	DC	CDS 3	1.3
5030	DC	CDS 3	52.1
5031	DC	CDS 3	94.2
5032	DC	CDS 3	40.2
5033	DC	CDS 3	86.3
5034	DC	CDS 3	80.5
5035	DC	CDS 3	167.9
5036	DC	CDS 3	164.9
5037	DC	CDS 3	256.9
5038	DC	CDS 3	260.0
5039	DC	CDS 3	312.7
5040	DC	CDS 3	311.8

Sample Locations (cont.)

Sample	Type (UG = underground) (DC = drill core)	Mine Level or Drill Hole	Elevation(m) (for UG) Depth(m) (for DC)
5041	DC	CDS 3	379.8
5043	DC	CDS 2	132.0
5044	DC	CDS 8	66.7
5045	DC	CDS 8	64.0
5046	DC	CDS 2	154.8
5047	DC	CDS 2	152.4
5048	DC	CDS 2	205.1
5049	DC	CDS 2	207.4
5050	DC	CDS 2	284.7
5051	DC	CDS 2	284.1
5052	DC	CDS 8	142.9
5053	DC	CDS 8	147.2
5054	DC	CDS 8	214.3
5055	DC	CDS 8	215.5
5056	DC	CDS 8	281.9
5057	DC	CDS 8	275.2
5058	DC	CDS 8	409.9
5059	DC	CDS 9	152.4
5060	DC	CDS 9	150.9
5061	DC	CDS 9	155.3
5062	DC	CDS 21	144.5
5063	DC	CDS 21	145.1
5064	DC	CDS 21	202.4
5065	DC	CDS 21	279.5
5066	DC	CDS 21	277.0
5067	DC	CDS 21	361.5
5068	DC	CDS 21	358.4

APPENDIX D

Fluid Inclusion Data

Table 3. Fluid inclusion homogenization temperatures and salinities.

Table 3. Fluid Inclusion Data

Sample	Elevation (m)	Homogenization Temperature (°C)	Salinity (eq.wt.% NaCl)
5025	3058	171	
5025	3058	181	6.4
5025	3058	190	
5025	3058	161	7.2
5025	3058	175	6.9
5025	3058	179	6.5
5025	3058	182	
5025	3058	189	6.0
5025	3058	201	
5025	3058	173	5.9
5025	3058	164	6.4
5025	3058	191	7.0
5025	3058	187	
5025	3058	185	7.5
5025	3058	197	7.2
5025	3058	194	
5025	3058	185	7.1
5025	3058	188	7.0
5025	3058	145	7.8
5025	3058	177	
5025	3058	183	8.1
5025	3058	169	7.6
5025	3058	170	
5025	3058	182	
5005	3157	207	6.3
5005	3157	168	
5005	3157	173	5.1
5005	3157	185	
5005	3157	187	5.5
5005	3157	183	6.0
5005	3157	179	
5005	3157	163	4.9
5006	3157	179	
5006	3157	181	6.1
5006	3157	161	
5006	3157	156	5.0
5006	3157	154	5.7
5006	3157	159	6.4

Table 3. Fluid Inclusion Data

Sample	Elevation (m)	Homogenization Temperature (°C)	Salinity (eq.wt.% NaCl)
5006	3157	163	6.3
5006	3157	157	
5015	2880	170	
5015	2880	149	
5015	2880	186	
5015	2880	237	
5015	2880	242	8.8
5015	2880	243	10.1
5015	2880	242	9.7
5015	2880	206	6.1
5015	2880	207	6.3
5015	2880	195	5.7
5015	2880	197	
5015	2880	187	5.0
5015	2880	189	7.0
5015	2880	187	
5015	2880	211	6.7
5015	2880	212	
5015	2880	211	
5015	2880	196	5.3
5015	2880	210	
5015	2880	215	
5015	2880	234	7.2
5015	2880	205	
5015	2880	209	5.8
5015	2880	207	
5015	2880	219	7.5
5015	2880	211	
5015	2880	233	
5015	2880	241	9.6
5016	2880	241	5.8
5016	2880	227	6.1
5016	2880	235	
5016	2880	236	
5016	2880	235	6.9
5016	2880	237	
5016	2880	231	
5016	2880	236	
5016	2880	237	8.3
5016	2880	235	7.9

Table 3. Fluid Inclusion Data

Sample	Elevation (m)	Homogenization Temperature (^{o}C)	Salinity (eq.wt.% NaCl)
5016	2880	238	7.5
5016	2880	238	
5016	2880	174	6.3
5016	2880	171	
5016	2880	170	5.9
5016	2880	221	
5016	2880	201	5.2
5016	2880	230	5.6
5016	2880	214	7.1
5016	2880	228	
5016	2880	241	
5016	2880	215	
5016	2880	212	
5016	2880	225	6.2
5016	2880	211	
5016	2880	212	6.1
5016	2880	207	5.9
5016	2880	216	5.9
5016	2880	211	
5016	2880	212	7.0
5016	2880	216	6.8
5016	2880	200	6.0
5016	2880	220	
5017	2880	209	6.3
5017	2880	237	7.9
5017	2880	242	
5017	2880	236	
5017	2880	236	6.9
5017	2880	236	
5017	2880	231	
5017	2880	232	5.8
5017	2880	233	5.9
5017	2880	228	6.4
5017	2880	230	
5017	2880	231	
5017	2880	233	

Table 3. Fluid Inclusion Data

Sample	Elevation (m)	Homogenization Temperature (°C)	Salinity (eq.wt.% NaCl)
5017	2880	235	7.9
5017	2880	207	6.4
5017	2880	200	
5017	2880	201	
5017	2880	202	
5017	2880	205	
5017	2880	207	6.5
5017	2880	263	7.7
5017	2880	248	6.8
5017	2880	235	8.1
5017	2880	173	
5017	2880	176	
5017	2880	171	5.2
5017	2880	173	
5017	2880	182	6.4
5017	2880	165	
5017	2880	190	
5017	2880	188	6.0
5017	2880	176	
5017	2880	215	7.0
5017	2880	215	6.6
5017	2880	217	
5017	2880	217	
5017	2880	217	
5017	2880	214	5.9
5017	2880	213	
5017	2880	216	7.1
5017	2880	211	6.6
5017	2880	212	6.5
5017	2880	206	5.4
5017	2880	217	6.7
5017	2880	220	
5017	2880	220	5.9
5017	2880	221	
5017	2880	220	
5017	2880	219	7.0
5017	2880	219	
5017	2880	218	6.1
5017	2880	220	

Table 3. Fluid Inclusion Data

Sample	Elevation (m)	Homogenization Temperature (°C)	Salinity (eq.wt.% NaCl)
5017	2880	220	
5017	2880	229	8.7
5017	2880	218	8.4
5017	2880	209	
5017	2880	211	6.8
5017	2880	210	
5017	2880	233	9.8
5017	2880	207	5.7
5017	2880	219	
5017	2880	218	7.3
5017	2880	217	
5017	2880	219	8.0
5017	2880	220	
5017	2880	219	6.5
5017	2880	219	7.2
5017	2880	220	
5017	2880	218	
5017	2880	220	7.3
5017	2880	220	7.1
5017	2880	221	6.9
5017	2880	220	
5017	2880	221	6.3
5017	2880	217	
5017	2880	220	7.2
5017	2880	219	
5017	2880	222	8.1
5010	2844	231	9.6
5010	2844	184	7.8
5010	2844	187	
5010	2844	191	
5010	2844	197	8.3
5010	2844	199	8.6
5010	2844	197	
5010	2844	207	8.9
5010	2844	213	
5010	2844	224	9.1
5010	2844	216	9.0
5010	2844	223	10.0
5010	2844	214	
5010	2844	215	

Table 3. Fluid Inclusion Data

Sample	Elevation (m)	Homogenization Temperature (°C)	Salinity (eq.wt.% NaCl)
5010	2844	213	
5010	2844	215	8.1
5010	2844	221	8.3
5010	2844	206	
5010	2844	220	
5010	2844	217	7.9
5010	2844	219	
5010	2844	217	9.4
5010	2844	210	9.5
5010	2844	207	
5012	2844	208	10.3
5012	2844	181	
5012	2844	176	
5012	2844	206	8.6
5012	2844	197	9.7
5012	2844	162	
5012	2844	198	8.1
5012	2844	194	8.5
5012	2844	219	11.0
5012	2844	186	
5012	2844	176	7.6
5012	2844	203	12.3
5012	2844	199	
5013	2844	201	
5013	2844	168	9.6
5013	2844	223	9.1
5013	2844	219	
5013	2844	221	10.1
5013	2844	217	8.9
5013	2844	221	
5013	2844	223	
5013	2844	216	9.4
5013	2844	218	9.8
5013	2844	216	
5013	2844	222	9.4
5013	2844	204	8.9
5013	2844	218	
5013	2844	219	8.1
5013	2844	204	
5013	2844	209	7.9

APPENDIX E

Atomic Absorption Data

Table 4. Concentrations of six metals in vein samples, determined by atomic absorption analysis.

Table 4. Atomic Absorption Data

Sample	Elevation (m)	Metal Concentration (wt.%)					
		Pb	Zn	Cu	Ag	Fe	Mn
5001	3156.8	0.04	0.76	0.003	0.0065	2.28	0.014
5002	3156.8	0.24	0.12	0.002	0.035	0.29	0.006
5003	3156.8	0.017	0.19	0.021	0.067	5.95	0.57
5004	3156.8	0.4	0.094	0.0094		0.07	0.009
5006	3156.8	0.72	0.007	0.01		0.19	0.0025
5008	3156.8		0.058	0.016			
5062	3129.5	1.39	0.0074	0.014	0.005	0.29	
5046	3107.8	0.3	0.54	0.36	0.077	0.23	
5052	3103.5	0.052	0.0075	0.0025	0.012	0.072	0.003
5028	3100.7	0.02	0.004	0.014			0.55
5025	3057.8	1.66	0.16	0.05	0.085	0.23	
5040	3006.9	1.84	0.003	0.023	0.045	0.11	0.017
5020	2935.8	0.022	0.029	0.0094	0.024	0.14	0.05
5021	2935.8	1.79	0.072	0.007	0.05	0.13	0.11
5022	2933.4	0.9	0.038	0.012	0.051	0.23	0.02
5023	2933.4	6.24	0.55	0.085	0.045	0.053	0.011
5024	2933.4	1.27	0.06	0.34	0.04	0.11	0.01
5015	2880.4	0.29	0.55	0.023	0.015	0.51	0.097
5017	2880.4	0.99	0.031	0.012	0.051	0.24	
5012	2844.1	3.35	0.2	0.0045	0.0094	0.21	0.04
5013	2844.1	1.61		0.042	0.045	0.17	0.012

REFERENCES

Barnes, H.L., 1979, Solubilities of ore minerals, in Barnes, H.L., ed., Geochemistry of hydrothermal ore deposits, 2nd ed.; John Wiley and Sons, Inc., 404-460.

Barton, P.B., Jr., Bethke, P.M., and Roedder, E., 1977, Environment of ore deposition in the Creede mining district, San Juan Mountains, Colorado: Part III: Progress toward interpretation of the chemistry of the ore forming fluid; Economic Geology, v.72, 1-24.

Barton, P.B., Jr., Bethke, P.M., and Toulmin, M.S., 1971, An attempt to determine the vertical component of flow rate of ore forming solutions in the OH vein, Creede, Colorado; Society of Mining Geologists of Japan, Special Issue 2, 132-136.

Bastin, E.S., 1941, Paragenetic relations in the silver ores of Zacatecas, Mexico; Economic Geology, v.36, 371-400.

Bastin, E.S., 1948, Mineral relationships in the ores of Pachuca and Real Del Monte, Hidalgo, Mexico; Economic Geology, v.43, 53-65.

Bastin, E.S., Graton, L.C., Lindgren, W., Newhouse, W.H., Schartz, G.M., and Short, M.N., 1931, Criteria of Age Relations of Minerals; Economic Geology, v.26, 561-610.

Berger, B.R., and Eimon, P.I., 1982, Comparative Models of Epithermal Silver-Gold Deposits, Society of Economic Geologists, Cameron Symposium, 25 pp.

Bethke, P.M., and Barton, P.B., Jr., 1971, History of filling of the OH vein, Creede, Colorado (abs.); Economic Geology, v.66, 1265.

Bethke, P.M., Barton, P.B., Jr., Lanphere, M.A., and Steven, T.A., 1976, Environment of ore deposition in the Creede mining district, San Juan Mountains, Colorado: Part II: Age of mineralization; Economic Geology, v.71, 1006-1011.

Bethke, P.M., Rye, R.O., and Barton, P.B., 1973, Hydrogen, oxygen, and sulfur isotopic compositions of ore fluids in the Creede district, Mineral County, Colorado (abs.); Economic Geology, v.68, 1205.

Bethke, P.M., and Rye, R.O., 1979, Environment of ore deposition in the Creede mining district, San Juan Mountains, Colorado: Part IV: Source of fluids from oxygen, hydrogen, and carbon isotope studies; Economic Geology, v.74, 1832-1851.

Bowers, T.S., Jackson, K.J., Helgeson, H.C., 1984, Equilibrium activity diagrams for coexisting minerals and aqueous solutions at pressures and temperatures to 5 kb and 600°C; Springer-Verlag, New York, 397 pp.

Colony, R.J., 1928, Ore-mineral sequence, in Fairbanks, E.E., The laboratory investigation of ores: A symposium; McGraw-Hill Book Co., New York, 262 pp.

Doe, B.R., Steven, T.A., Delevaux, M.H., Stacey, J.S., Lipman, P.W., and Fisher, F.S., 1979, Genesis of ore deposits in the San Juan volcanic field, southwestern Colorado; Economic Geology, v.74, 1-26.

Giudice, P.M., 1980, Mineralization at the convergence of the Amethyst and OH fault systems, Creede district, Mineral County, Colorado; M.S. Thesis, University of Arizona, 95 pp.

Goodspeed, G.E., 1936, Microstructures and metallization of the gold-quartz veins of Cornucopia, Oregon; Economic Geology, v.31, 398-416.

Helgeson, H.C., 1969, Thermodynamics of hydrothermal systems at elevated temperatures and pressures; American Journal of Science, v.267, 729-804.

Henley, R.W., Truesdell, A.H., and Barton, P.B., Jr., 1984, Fluid mineral equilibria in hydrothermal systems; Economic Geology Publishing Co., El Paso, 267 pp.

Lindgren, W., 1933, Mineral Deposits, 4th Ed.; McGraw-Hill Book Co., New York, 371 pp.

Lindgren, W., 1935, The silver mine at Colquijirca, Peru; Economic Geology, v.30, 331-346.

Lipman, P.W., 1975, Evolution of the Platoro Caldera complex and related volcanic rocks, southwestern San Juan Mountains, Colorado; U.S.G.S. Professional Paper 852, 128 pp.

Lipman, P.W., 1979, Emplacement of high-level granite batholiths: Evidence from the San Juan volcanic field of Colorado and the Boulder batholith of Montana, (abs.); G.S.A. Abstracts with Programs, v.11, 467.

Lipman, P.W., Fisher, F.S., Mehnert, H.H., Naeser, C.W., Luedke, R.G., and Steven, T.A., 1976, Multiple ages of mid-Tertiary mineralization and alteration in the western San Juan Mountains, Colorado; Economic Geology, v.71, 571-588.

Robinson, R.W., and Norman, D.I., 1984, Mineralogy and fluid inclusion study of the southern Amethyst vein system, Creede mining district, Colorado; Economic Geology, v.79, 439-447.

Roedder, Edwin, 1960, Primary fluid inclusions in spalerite crystals from the OH vein, Creede, Colorado; Geological Society of America Bulletin, v.71, 1958.

Roedder, Edwin, 1974, Changes in ore fluids with time, from fluid inclusion studies at Creede, Colorado; 4th Symposium of the I.A.G.O.D., Varna, v.II, 179-185.

Seward, T.M., 1976, The stability of chloride complexes of silver in hydrothermal solutions up to 350°C; Geochimica et Cosmochimica Acta, v.40, 1329-1341.

Seward, T.M., 1984, The formation of lead(II) chloride complexes to 300°C; A spectrophotometric study; Geochimica and Cosmochimica Acta, v.48, 121-134.

Steven, T.A., and Eaton, G.P., 1975, Environment of ore deposition in the Creede mining district, San Juan Mountains, Colorado: Part I: Geologic, hydrologic, and geophysical setting; Economic Geology, v.70, 1023-1037.

Weissberg, B.G., Browne, P.R.L., and Seward, T.M., 1979, Ore metals in active geothermal systems, in Barnes, H.L., ed., Geochemistry of hydrothermal ore deposits: 2nd ed.; John Wiley and Sons, Inc., New York, 738-780.

This thesis is accepted on behalf of the faculty of the Institute by the following committee:

David L. Norman
Advisor

Paul L. Emion

Andrew Campbell

2 April 1986
Date